Tova Neustadt Schachter

Graduate Research Assistant, Department of Biochemistry and Molecular Biology

University of Maryland School of Medicine

Biomedical Research Facility

108 N Greene Street Room 227

Baltimore, MD 21201

Phone: 410-706-5787

Email: tovas22@gmail.com

Education

2006-present PhD candidate, Department of Biochemistry and Molecular Biology

University of Maryland School of Medicine, Baltimore, MD

Advisor: Martin F Schneider Ph.D.

Thesis: **The control and effects of Foxo1 in skeletal muscle**

2005 B.S. in Biology

Touro College, Brooklyn, NY

Research Experience

2006-present **Graduate Research Assistant**, Dept of Biochemistry and Molecular Biology

University of Maryland School of Medicine, Baltimore MD

P.I. Dr. M. Schneider

- Working to calculate the rates of import and export of the transcription factor Foxo1. This will elucidate the effects of activating-kinase inactivity as well as the timescale on which these effects occur.

- Techniques utilized: cell culture, muscle isolation, virus infection of cells and fiber, confocal microscopy, virus amplification, transformation and transfection

2006 **Graduate Lab Rotation**, Dept of Inorganic Chemistry and Biochemistry

University of Maryland Baltimore County (UMBC)

P.I. Dr. V. Szalai

- Research to find conditions under which specific oligonucleotides would form guanine quadruplexes and stack with metalloporphyrins.
- Using spectroscopy of titrations with changes in porphyrin, oligo concentration, and salts the maximum concentration of bound porphyrin was attained.

2005 **Lab of Retroviral Immunology**, The Public Health Research Institute-UMDNJ

P.I. Dr. A. Pinter

- Isolation of recombinant proteins and antibodies
- Cultured cells that secreted proteins necessary in experimentation on the HIV-1 viral strains and then purified them
- Techniques used: ELISA, SDS-PAGE, Spectrophotometry

ABSTRACT

Title of Dissertation: The control and effects of Foxo1 in skeletal muscle

Tova Neustadt Schachter, Doctor of Philosophy, 2012

Dissertation Directed by: Martin F. Schneider, Ph.D., Professor, Department of Biochemistry and Molecular Biology

In skeletal muscle, the transcription factors Foxo1 and Foxo3A control expression of proteins which mediate muscle atrophy, making the nuclear concentration and nuclear/cytoplasmic movements of Foxo1 and Foxo3A of therapeutic interest in conditions of muscle wasting. Here, we use Foxo-GFP fusion proteins adenovirally expressed in cultured adult mouse skeletal muscle fibers to characterize the time course of nuclear efflux of Foxo1-GFP in response to activation of the IGF-1/PI3K/Akt pathway, to determine the time course of nuclear influx of Foxo1-GFP during inhibition of this pathway, and to explore the effects of Foxo1 on contraction of muscle fibers. Localization of endogenous Foxo1 in muscle fibers, as determined via immunocytochemistry, is consistent with that of Foxo1-GFP. Inhibition of the nuclear export carrier CRM1 by Leptomycin B (LMB) traps Foxo1 in the nucleus and results in a relatively rapid rate of Foxo1 nuclear accumulation, consistent with a high rate of nuclear/cytoplasmic shuttling of Foxo1 under control conditions prior to LMB application, with near balance of unidirectional influx and efflux. Expressed Foxo3A-GFP shuttles about 20 fold more slowly than Foxo1-GFP. Fibers expressing Foxo1-GFP exhibit an inability to contract, abnormal propagation of action potentials, and ablation of

calcium transients in response to electrical stimulation compared to fibers expressing GFP alone. Evaluation of the T-tubule system, the membranous system involved in the radial and longitudinal propagation of the action potential, using a membrane fluorescent dye, revealed an intact T-tubule network in fibers over-expressing Foxo1-GFP. Interestingly, long-term IGF-1 treatment in Foxo1-GFP fibers induced recovery of normal calcium transients, indicating that Foxo1 translocation affects the expression of proteins involved in the generation and/or propagation of action potentials. A decrease in Nav1.4 expression in fibers overexpressing Foxo1 was also observed in the absence of IGF-1. We conclude that overactivity of Foxo1 prevents the normal muscle responses to electrical stimulation by decreasing expression of Nav1.4 and possibly other means. Our approach allows quantitative kinetic characterization of Foxo1 and Foxo3A nuclear-cytoplasmic movements in living muscle fibers under various experimental conditions, as well as the effects of Foxo1 on the electrophysiology of muscle.

The control and effects of Foxo1 in skeletal muscle

By

Tova Neustadt Schachter

Dissertation submitted to the faculty of the Graduate School of the
University of Maryland, Baltimore in partial fulfillment
of the requirements for the degree of
Doctor of Philosophy
2012

Dedication

To my husband, Shmuel, who has sacrificed so much to help me reach this accomplishment.

To my kids, Rochel, Sara, and Mordechai, this is for you!

To my parents, my siblings and their families, and my husband's parents and family: your support (and help) has kept me going. Thank you.

To my neighbors and friends who always come through- babysitting, food, encouragement, and a listening ear.

Acknowledgements

First, I must thank my advisor, Dr. Martin Schneider, with whom it is always a pleasure to work. I am forever changed by your example as a boss, a scientist, a collaborator, and a person. You have taught me so much science, and so much more.

The Schneider lab is a great place to work. Thank you so much to all of my lab mates who have helped me in so many ways. Tiansheng Shen trained me in so many of the techniques that I use and has advised me and brainstormed with me throughout my time as a graduate student. Erick Hernández-Ochoa has an unbelievable wealth of knowledge and technical experience that he has been so kind to share with me whenever I need help (the range is absolutely astonishing). Minerva Contreras taught me so much when I joined the lab and was so patient and easy to work with. Pat Robison is always ready to help me brainstorm and think out of the box. Thank you to Yewei Liu, Rob Wimmer, Jeremiah Brown, and Rotimi Olojo and all of my lab mates over the years who have been a pleasure to work with and have helped me get to this point.

I cannot thank my doctoral committee enough: Drs. Martin Schneider, Bill Randall, Katia Kontrogianni, Paul Smith, and Iain Farrance. Your guidance and kindness have been beyond measure. It is an honor to have such an accomplished and well respected committee.

Thank you to the Meyerhoff family for more than I can say.

Thank you to the entire staff of the Biochemistry and Molecular Biology department, especially Kathleen, Koula, Heather, and Kim.

When Dr. Joseph Hill of University of Texas Southwestern Medical Center gifted the Schneider lab with an adenovirus encoding Foxo1-GFP, I am sure that he did not envision my dissertation. I am never-the-less grateful to him.

Table of Contents

List of Figures

CHAPTER 1

INTRODUCTION

A. Background

The Forkhead box (Fox) transcription superfamily is evolutionarily conserved. In 1989, the first member of this superfamily, the *fork head* gene, in *Drosophila melanogaster* was identified. Mutation of the *fork head* gene results in a distinct forkhead-like appearance of *Drosophila melanogaster*, giving rise to the name of the transcription factor superfamily (1). Since then, over 100 transcription factors containing a 100-residue DNA-binding domain termed the forkhead domain have been identified, and so, in 2000, a new inclusive nomenclature system was developed. The Foxo class is mammalian and, in terms of homology of the forkhead domain, the most diverse of all Fox classes.

Foxo1 (previously known as forkhead homolog in rhabdomyosarcomas; FKHR) was first identified in alveolar rhabdomyosarcomas as the product of a chromosomal translocation

in which the N-terminal portion of Pax3 was fused to the C-terminal portion of Foxo1, including a truncated portion of the forkhead domain (2).

B. Structure

All members of the Fox superfamily share a common 100-residue DNA-binding domain known as the forkhead domain. This domain has three major α-helices as well as two large wing-like loops, which gave rise to a second name for this group of transcription factors: winged helix transcription factors (3, 4). The third helix (H3) and both loop regions associate with the DNA cognate recognition sequence, [(T/A) (A/T) A A C A] (4, 5).

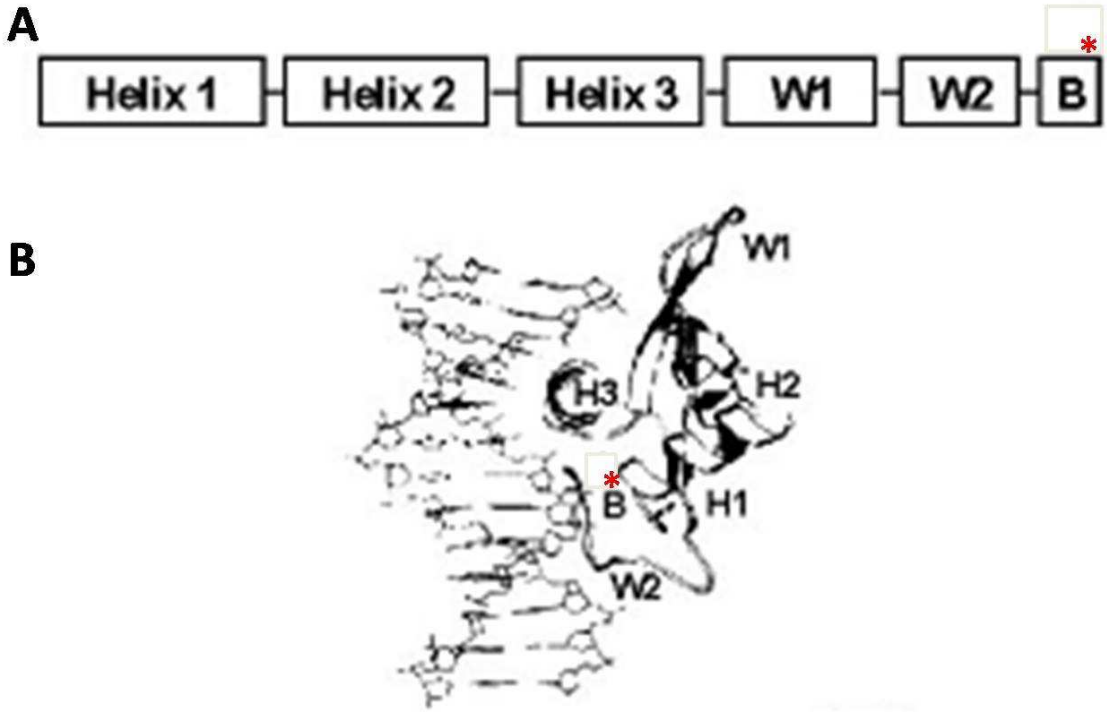

Figure 1.1 The "winged helix" secondary and tertiary structures of the DNA-binding forkhead domain of Forkhead box transcription factors during interaction with DNA.

(A) The forkhead domain consists of three N-terminal α-helices, H1, H2, and H3, two wing-like structures, W1 and W2, and a C-terminal basic region (B). The * in the C-terminal basic region signifies the critical serine 256 in Foxo1 (corresponding to serine 253 in Foxo3 and serine 193 in Foxo4) that is phosphorylated by Akt. This basic region (B) located within the DNA binding domain (DBD) may interact with the phosphate backbone of DNA to increase stability of the complex in a sequence non-specific manner. (B) The third helix, H3, in the forkhead domain directly interacts with DNA, whereas H1, H2, and the two wing-like structures W1 and W2 are not directly involved with DNA binding. This figure has been modified from Zhang et al., 2002 (15).

Phosphorylation of Foxo prevents its nuclear localization and thus DNA binding, thereby inhibiting the transcription of atrogenes, genes for proteins that cause muscle atrophy. There are three highly conserved Akt (also known as protein kinase B; PKB) phosphorylation sites Thr-24, Ser-256, and Ser-319 in human FOXO1 (6-8).

Although the primary regulation of Foxo occurs through Akt-mediated phosphorylation, serum- and glucocorticoid-inducible kinase (SGK) also has the ability to phosphorylate these residues (9). Casein kinase 1 (CK1), DYRK1A, and other kinases have different recognized phosphorylation sites (10-12). While phosphorylation via various kinases causes cytoplasmic retention, it stands to reason that dephosphorylation via phosphatases induce nuclear influx of Foxo. To date, the only phosphatase that has been shown to directly dephosphorylate Foxo is the serine/threonine phosphatase PP2A (13). Okadaic acid (OA), a PP2A inhibitor, prevents this dephosphorylation, thereby inhibiting the nuclear influx of Foxo1 (14).

There are differences in function between the three residues which Akt phosphorylates. SGK preferentially phosphorylates S319, whereas Akt preferentially phosphorylates S256 (9). S256 is located in a basic region at the C-terminal end of the DNA binding domain (DBD) that may increase stability of DNA-Foxo interaction and has been shown to function as a nuclear localization signal (15). S256 must be phosphorylated first in order for phosphorylation of T24 and S319 to occur. However, phosphorylated S256 alone is not sufficient to prevent nuclear translocation, but it is sufficient to disrupt DNA-Foxo interaction independently (15, 16). This functional aspect of S256 on Foxo1 corresponds well with the structural understanding of Foxo1 and the stability of Foxo-DNA interaction due to the basic region of the forkhead domain in which S256 is located (see **Figure 1.1**).

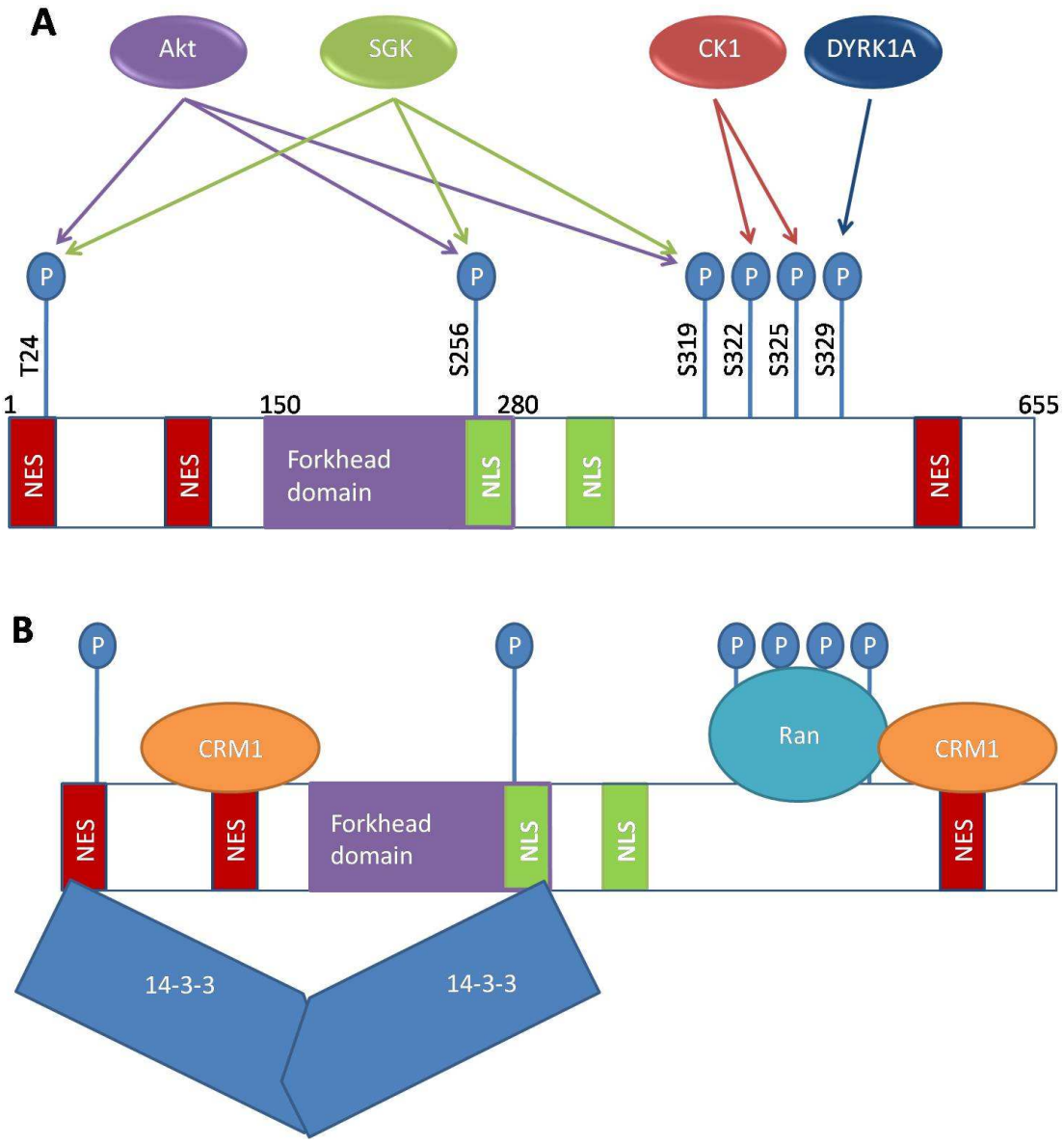

Figure 1.2 Functional domains of Foxo1.

(**A**) Nuclear import and export of Foxo1 is regulated by Foxo1 kinases include Akt, SGK, CK1, and DYRK1A. Foxo1 is 655 amino acids long and contains 2 nuclear localizing sequences (NLS) and 3 nuclear export sequences (NES). (**B**) CRM1 binds to the C-terminal NES and interacts with the Ran complex which binds to an acidic patch of phosphorylated serines. The NES directly N-terminal to the forkhead domain also binds CRM1. The nuclear localization is further regulated by the cooperative binding of a 14-3-3 dimer between the N-terminal NES and an NLS.

C-terminal to the DBD is a leucine-rich nuclear export signal (NES). Nuclear export of Foxo1 is inhibited by leptomycin B, indicating its interaction with chromosome region maintenance 1 (CRM1), a nuclear export protein (17). Indeed, CRM1 binds to the C-terminal NES and the NES located N-terminal to the DBD, but not to the N-terminal NES. Interestingly, CRM1 binding and subsequent nuclear export seem to be unaffected by Foxo's phosphorylation status (18).

Between the DBD and the CRM1 binding site is situated an acidic patch of serines which are phosphorylated under some conditions. S319 is phosphorylated by Akt whereas S322 and S325 are phosphorylated by CK1 and S329 is phosphorylated by DYRK1A (**Figure 1.2**). This acidic patch increases the rate of nuclear import via interaction with the Ran protein complex (10).

Mutation studies have been important in determining the residues critical to nuclear-cytopalsmic localization of Foxo1. Zhang et al., 2002, employed plasmids containing wild type Foxo1-GFP as well as plasmids containing point mutations in Foxo1-GFP. The mutation S256A caused nuclear localization, whereas the mutation S256D caused nuclear exclusion of Foxo1, demonstrating the necessity of phosphorylation at this site for nuclear exclusion. In order to determine whether this is due to the effect that S256 has on the phosphorylation status of T24 and S319 or due to other effects, constructs were made with T24A- S319A and with T24A-S256D-S319A. T24A- S319A caused nuclear targeting and the addition of a negative charge at 256 in making T24A-S256D-S319A did not disrupt this nuclear targeting. Taken together, these data indicate that the nuclear exclusion that results from phosphorylation of S256 is mediated via phosphorylation of

T24 and S319. Furthermore, mutation of S256D was insufficient to prevent the function of the NLS region in which it is located (15).

Decrease in transactivation of target genes by Foxo1 in response to IGF-1 treatment, as determined using a luciferase reporter gene construct, showed phosphorylation of S256 to be necessary for induction of expression of downstream atrogenes. However, mutation of S256 to an alanine targets Foxo1 to the nucleus, indicating that DNA binding is dependent on more than nuclear-cytoplasmic localization. Foxo1-DNA binding is dependent on characteristics of Foxo1 that are affected by phosphorylation of S256 as well, such as phosphorylation of T24 and S319 (**Figure 1.3**, reference 15).

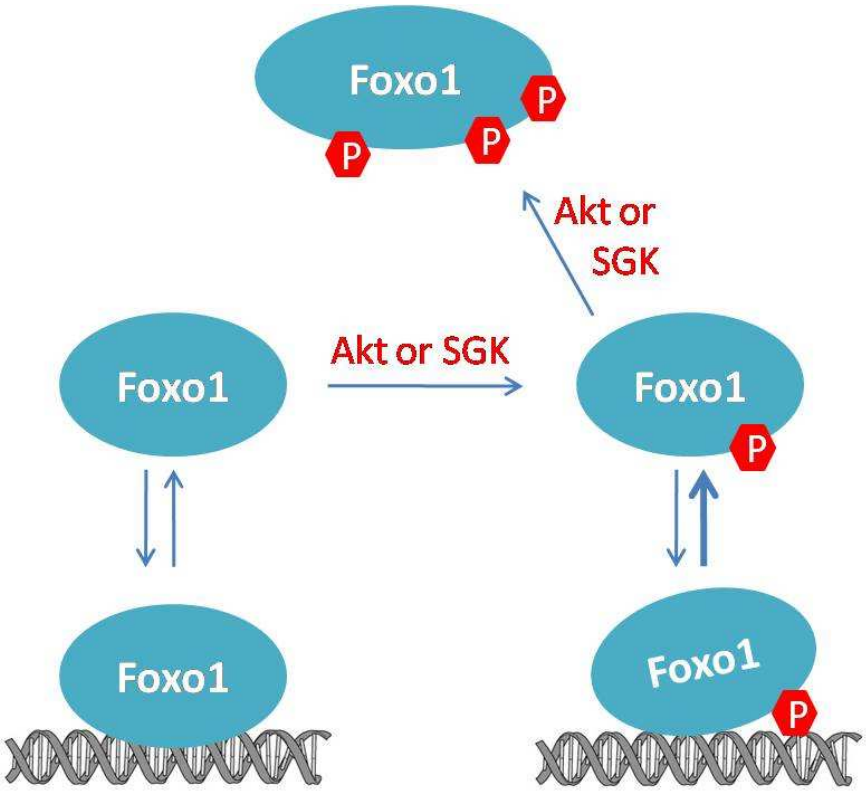

Figure 1.3 Model of possible mechanism for disruption of Foxo1-DNA interaction by phosphorylation of S256. This model also accounts for the increase in phosphorylation of T24 and S319 that occurs when S256 is phosphorylated.

C. Regulation

Regulation of Foxo-mediated muscle atrophy occurs through the IGF/Akt/PI3K pathway (**Figure 1.4**). Atrophy caused by overexpression of Foxo3A in both C2C12 myotubes and tibialis anterior fibers was inhibited by IGF treatment or by overexpression of Akt (19), whereas treatment of muscle cells with IGF-1 promoted hypertrophy (20). While this pathway is integral to Foxo signaling, other post-transcriptional modifications affect Foxo activity. Acetylation, ubiquitination, and phosphorylation via other proteins also regulate Foxo's ability to induce expression of target genes.

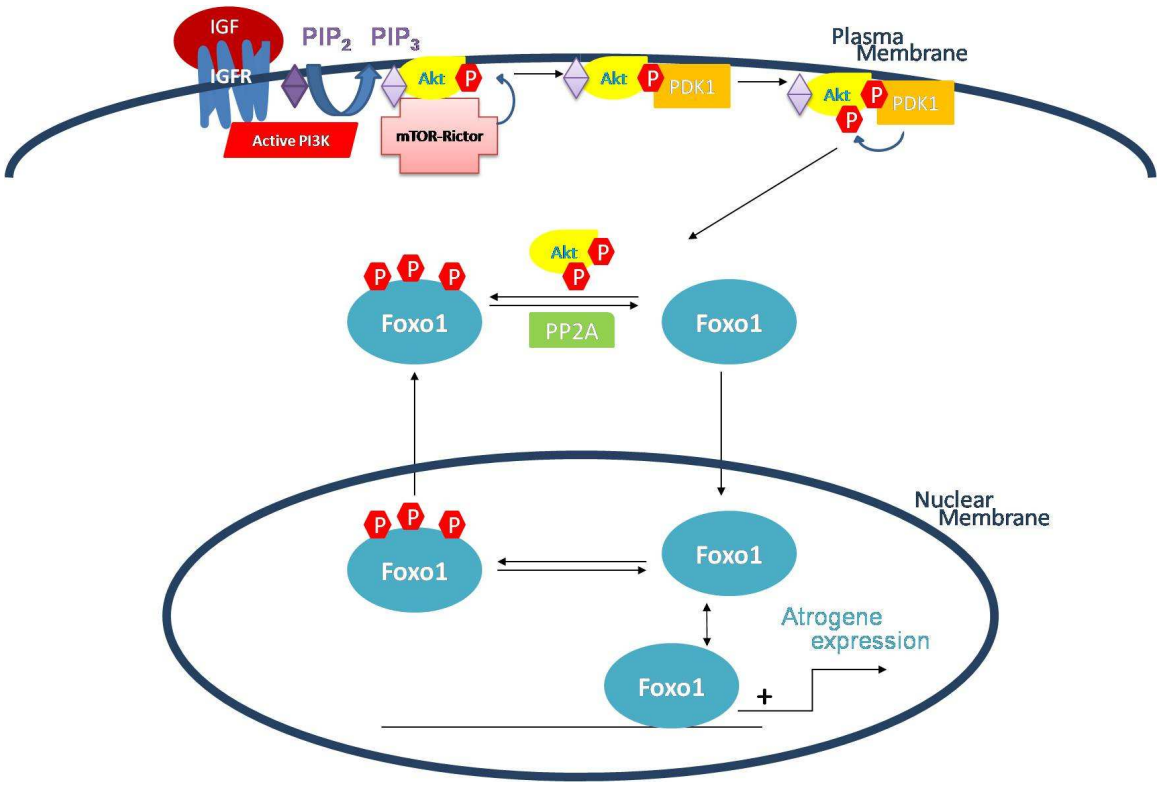

Figure 1.4 Foxo1 nuclear import and export pathway.

Insulin like growth factor (IGF) binds to its membrane-bound receptor (IGFR), thereby activating PI3K which converts PIP_2 to PIP_3. Akt binds to PIP_3, where it is phosphorylated by the mTOR-Rictor complex and PDK1. Phosphorylated Akt acts as a kinase and directly phosphorylates Foxo1. Foxo1 which has been phosphorylated is excluded from the nucleus. PP2A can directly dephosphorylate Foxo1, thus driving nuclear import.

1. IGF/Akt/PI3K pathway

The pathway that leads to cytoplasmic retention of Foxo begins when a growth stimulus, such as IGF- (insulin-like growth factor) 1, platelet-derived growth factor (PDGF), epidermal growth factor (EGF), insulin, thrombin, or nerve growth factor (NGF), binds to

its respective membrane-bound receptor and activates phosphatidylinositol-3-kinase (21, 22). PI3K phosphorylates phosphatidylinositol-4,5-bisphosphate (PIP_2), converting it to phosphatidylinositol-3,4,5-trisphosphate (PIP_3), which forms a lipid binding site on the cell membrane for Akt, a serine/threonine kinase. At the membrane, Akt is activated via phosphorylation by the kinase phosphoinoside-dependent kinase 1 (21, 23). Akt-mediated phosphorylation of Foxo1 leads to nuclear exclusion and deactivation of Foxo1 (24). This effect is mediated through mTORC2 (which contains Rictor) and not through rapamycin (25).

2. Serum and glucocorticoid-inducible kinase

Another kinase which is structurally related to Akt and phosphorylates Foxo is serum and glucocorticoid-inducible kinase (SGK; reference 9). Like Akt, SGK is phosphorylated by PDK1 and PI3K and then phosphorylates Foxo (26). Akt and SGK have the same putative binding sequence and can phosphorylate the same residues on Foxo. However, experiments have shown that Akt preferentially phosphorylates S256 whereas SGK preferentially phosphorylates S319 (9). However, Akt does phosphorylate S319, indicating that Akt may be able to compensate for SGK (27).

3. Casein Kinase 1

Casein Kinase (CK1) is a serine/threonine kinase that is negatively regulated by autophosphorylation (28). CK1 phosphorylates Foxo1 at S319 and S322 after it has already been phosphorylated at S316 (10, 29). Phosphorylation of S319 is a precursor to S322 phosphorylation by CK1. In PDK1 embryonic knockout cells (which are used to further determine the role of Akt in various pathways because they fail to phosphorylate

and thus activate Akt), no phosphorylation of Foxo on the Akt phosphorylation sites or CK1 sites (S319 and S322) occurred, clearly demonstrating the dependence of CK1 phosphorylation of Foxo1 on priming by Akt (10).

4. DYRK1A

DYRK kinases are also serine/threonine kinases that are regulated by autophosphorylation (30). DYRK1A phosphorylates Foxo1 at S329, which, together with the residues S316, S319, and S322 phosphorylated by Akt and CK1 (**Figure 1.2**), create an acidic patch. This acidic patch increases the rate of nuclear import via interaction with the Ran protein complex (10).

5. Ras-Ral

The Ras-Ral signaling pathway has been shown to influence Foxo4's transactivational capacity but not its nuclear-cytoplasmic localization. However, this pathway has as of yet not been shown to affect other Foxo transcription factors, and its involvement is particularly questionable due to a low degree of conservation of the Ral-dependent phosphorylation sites (31).

6. 14-3-3

14-3-3 binds cooperatively to an NLS and NES on Foxo as a dimer and assists in its nuclear export (12, 17). When Foxo3A is bound to 14-3-3, dephosphorylation by PP2A of Foxo3A at T32 and S253 (T24 and S256 on Foxo1) is decreased. However, dephosphorylation of these sites by PP2A is necessary for dissociation of 14-3-3 from Foxo, nuclear import, and expression of target genes, indicating that these phosphorylated

residues act as docking sites for 14-3-3 (13). There is also evidence that increased 14-3-3 binding increases Foxo degradation, presumably by maintaining Foxo in the cytoplasm where it can be tagged by ubiquitin.

7. PP2A

To date, PP2A is the only known phosphatase that directly dephosphorylates Foxo. This finding is particularly significant to our understanding of Foxo1 regulation in that it demonstrates the dynamic dual direction of phosphorylation. (13).

8. Acetylation

In healthy cells, Foxo is predominantly in the cytoplasm. Stress inducers, such as low concentration H_2O_2, can stimulate nuclear translocation and Foxo1 regulation in a manner that is not sensitive to growth factors. It is interesting to note that stress-induced acetylation does not affect growth factor-induced Akt (or SGK) phosphorylation and stress-induced nuclear targeting overrides the cytoplasmic retention that would normally result from Foxo phosphorylation (32). Oxidative stress leads to association with p300/CREB-binding protein (CBP) and p300/CBP-associated factor (PCAF), which leads to acetylation of Foxo4 at K186, K189, and K408 (33). These acetylation residues are primarily in the DBD, indicating that acetylation likely regulates DNA binding. This hypothesis was confirmed through further experimentation which demonstrated that deacetylation of Foxo by Sirt1 inhibits its transactivational activity and prevents cell apoptosis (32, 34).

9. Ubiquitination and proteasomal degradation

Cytoplasmic Foxo1 phosphorylation leads to ubiquitination and subsequent proteasomal degradation (35). However, over the 2-4 hour time period of the studies shown in this work, negligible change in the cytoplasmic fluorescence occurred (**Figure 1.5**). Skp2, a member of the SCF ubiquitin ligase complexes, has been identified as the ubiquitin ligase that ubiquitinates Foxo1. Phosphorylation of S256 on Foxo1 is a necessary precursor to Skp2-induced ubiquitination and thus induces proteasomal degradation of Foxo1. Foxo1 ubiquitination results in decreased total Foxo1 in the cell due to proteasomal degradation and is thus a mechanism for reducing Foxo1 activity (36). Discussion of proteasomal degradation will continue in further detail in the *Muscle atrophy* section of *Role of Foxo in muscle*.

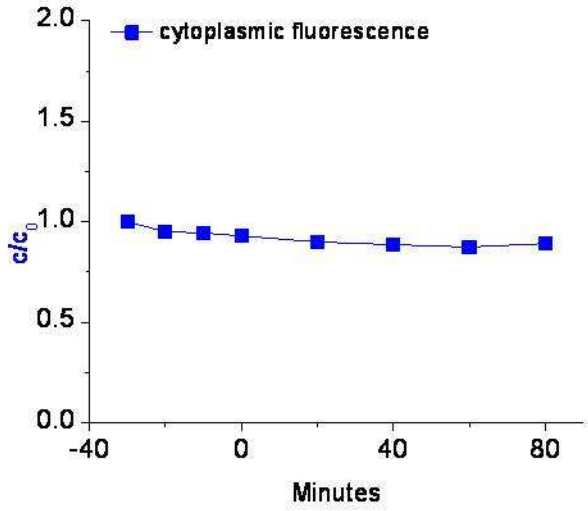

Figure 1.5 Cytoplasmic Foxo1-GFP expression does not change during experiments. Degradation of Foxo1 is not detectable during experiments.

D. Foxo isoforms

Four members of the forkhead transcription factor family are found in humans; Foxo1 (FKHR), Foxo3A (FKHRL), Foxo4 (AFX), and Foxo6. Foxo1, Foxo3, and Foxo4 are all expressed in skeletal muscle, however Foxo6 is expressed mainly in the brain and is not present in muscle (37). In adult mice, Foxo1 is expressed in many tissue types, but most strongly in ovary and uterus tissue. Foxo3 (the murine ortholog of Foxo3A) is expressed in all tissue types studied in Biggs et al., 2001, whereas Foxo4 is expressed only in skeletal muscle (5). Moreover, Foxo1 and Foxo3A are the forkhead transcription factors associated with muscle atrophy, and upregulation of either one individually has been shown to be sufficient to induce muscle atrophy (19, 38).

Human Foxo transcription factors and their murine orthologs have very high homology. In their forkhead domains Foxo1 and Foxo3A are 100% identical to their murine orthologs, and Foxo4 is 96% identical. Over their entire lengths, their homology decreases but is still very high. Foxo1 has 91%, Foxo3A has 94%, and Foxo4 has 86% identity to their respective murine orthologs (5).

Despite their homology, the functions of Foxo transcription factors seem to be diverse. By developing knockout mice of each isoform, the unique function of each Foxo transcription factor has been made clearer. *Foxo1* knockout mice were embryonic lethal. Development of the vasculature of the yolk sack was diminished in comparison to control fetuses indicating that Foxo1 is an essential regulator of embryonic vessel formation. Furthermore, Foxo1 showed a high level of expression in developing vessels, and the physiological and temporal location of Foxo1 suggests that Foxo1 plays an important role

in the process of embryonic angiogenesis. *Foxo3a*-null mice had age-dependent reduced fertility, indicating that Foxo3A is necessary for ovarian follicular development. Interestingly, *Foxo4*-null mice did not exhibit any noticeable phenotype. Hosaka et al., suggest that it is possible that *Foxo4*-null mice may not respond normally to specific treatments which have not yet been determined or tested (39). Moylan et al, established a function of Foxo4. In C2C12 myotubes, Foxo4 was shown to mediate the upregulation of atrogin induced by tumor necrosis factor (TNF). IGF/Akt/Foxo signaling was intact, but Foxo1 and Foxo3 were not affected by TNF treatment. The only Foxo transcription factor affected by TNF was Foxo4 (40).

There is evidence that the different Foxo isoforms are all regulated in the same ways and that they regulate transactivation in a redundant manner. For instance, Foxo1, Foxo3A, and Foxo4 are all phosphorylated by Akt (5, 7, 41, 42). In C2C12 cells that had been starved or treated with the synthetic glucocorticoid dexamethasone, two models of myotube atrophy, Foxo1, Foxo3, and Foxo4 all appeared to be phosphorylated and dephosphorylated in a similar manner. Furthermore, the function of Foxo1 and Foxo4 were reduced by expression of dominant negative Foxo3A (19). In vivo, Foxo1 and Foxo3 also seem to respond similar to each other. In the diaphragms of 12- and 24-month old mice, nuclear Foxo1 and Foxo3A were decreased in comparison to the nuclear Foxo1 and Foxo3A found in the diaphragms of 2-month old mice. However, Foxo4 nuclear presence remained the same, indicating that Foxo1, Foxo3A, and Foxo4 are not completely redundant and are in part regulated differently (43).

More recently, differences in both the function and regulation of the Foxo transcription factors have been highlighted. Both Foxo1 and Foxo3a respond to nerve growth factor

(NGF) with nuclear efflux, but Foxo3A has been shown to be more sensitive to NGF than Foxo1 in PC12 cells. Consistent with this, Foxo3A nuclear export occurred at a higher rate than that of Foxo1 (44).

In skeletal muscle, the similarities and differences between expression of Foxo transcription factors were examined in depth. Expression of Foxo1 and Foxo3 was upregulated in mouse gastrocnemius during starvation. Foxo1 gene expression increased noticeably at 6 hours and peaked at 12 hours of starvation, returning to normal after 24 hours of refeeding. Foxo3 mRNA increased noticeably at 6 hours of starvation but did not peak until 24 hours of starvation and also returned to normal levels after 24 hours of refeeding. Only a small change was seen in Foxo4 gene expression during starvation and refeeding. During starvation, blood-glucocorticoid levels increase. In response to glucocorticoid treatment, Foxo1 expression increased three-fold whereas Foxo3 and Foxo4 increased only slightly (1.3- and 1.6-fold respectively). These results indicate that elevated glucocorticoids are sufficient to induce an increase in expression of Foxo isoforms to differing extents and are possibly directly responsible for the increase in Foxo expression in skeletal muscle that results from starvation (45).

In summary, Foxo isoforms have similar DNA binding domains (DBD) and consensus binding sites, but not the same functions, as clearly demonstrated by the differences in phenotype of Foxo1, Foxo3A, and Foxo4 knockout mice (5, 39). Overall, based on the diverse functions and differences in regulation, the Foxo proteins do not appear to be redundant. How are the isoforms induced to regulate their different functions? One answer is possibly difference in cell-type expression levels. Another answer is binding partners that increase specificity or inhibit binding to specific promoter regions. A third

possibility is that specific combinations of post-transcriptional modifications promote specific functions over others. It is likely that a combination of the mentioned regulators and/or other factors control specificity of Foxo-induced protein expression.

E. Function

Transcription factors from the forkhead family possess diverse function. Foxo is a major player in many vital cellular functions such as cell proliferation, cell cycle, and cellular survival (6, 24, 46, 47). In fact, Foxo1 is crucial to fetal development, and Foxo1 knockout mice are embryonic lethal (39, 48). The importance of Foxo1 was also demonstrated using cre-mediated disruption of Foxo1 expression, thereby demonstrating its function as a tumor suppressor (39, 48). Another example of crucial regulation by a forkhead family member is the athymic immunodeficient *nude* mouse. This phenotype is due to a mutation in *winged helix nude* (49).

F. Roles of Foxo in muscle

While the role of Foxo transcription factors in muscle is somewhat diverse- including regulation of muscle differentiation, glucose metabolism, angiogenesis, and skeletal muscle fiber type remodeling - its recognized primary importance is regulation of muscle atrophy. Overexpression of Foxo1 in skeletal muscle results in decreased muscle size, decreased number of type I fibers, and impaired skeletal muscle function (38). In addition, expression of Foxo1 is upregulated after fasting and under other stress

conditions in skeletal muscle (50). Muscle atrophy, also referred to as muscle wasting, is characterized by a decrease in muscle mass due to a decrease in the size of muscle fibers, not the number of fibers. Muscle atrophy results from bed rest, disuse, denervation, diseases such as AIDS and various forms of cancer, sepsis, and aging. Therefore, skeletal muscle is a beneficial system in which to develop a Foxo1 model. Here, we will briefly review the structure of skeletal muscle and then highlight the roles of Foxo in skeletal muscle as well as in smooth muscle.

1. Skeltelal muscle structure and muscle differentiation

Skeletal muscle fibers are striated and polynucleated, with nuclei generally located on the periphery (**Figure 1.6**). Flexor digitorum brevis (FDB) is composed primarily of fast twitch fibers.

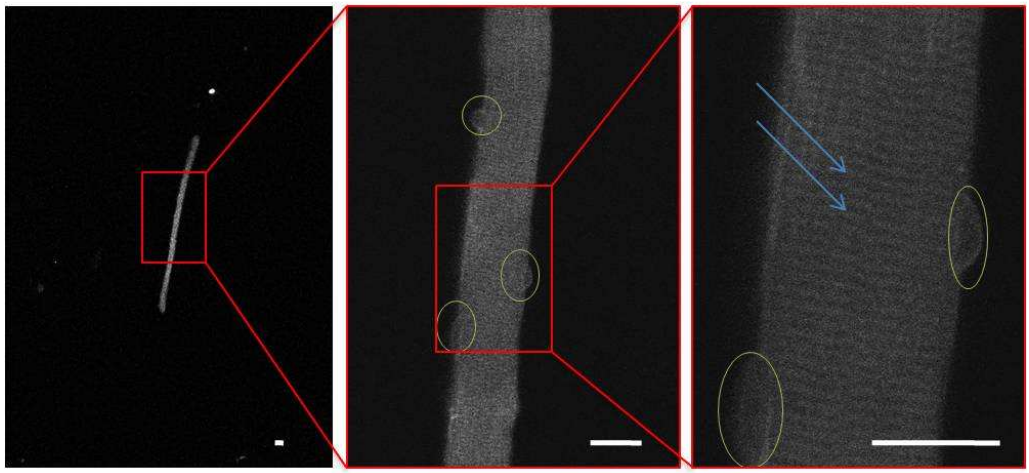

Figure 1.6 FDB fiber at different magnification.

Striations are denoted with blue arrows and nuclei are identified with green circles. Scale bars are 20 μm.

Foxo1 regulates the rate of fusion of differentiating primary myotubes and it targets the nucleus in myoblast differentiation in a manner that is Akt-dependent (24, 51). Foxo1 also affects muscle type expression. In mice, overexpression of Foxo1 in skeletal muscle resulted in muscles that were whiter in color, indicating a decrease in slow-twitch muscles fibers. In fact, histological studies showed a significant decrease in slow-twitch fibers. Furthermore, these mice had decreased running wheel activity, indicating decreased endurance, consistent with reduced slow-twitch fiber expression (38).

2. Glucose metabolism

Muscle is the most abundant tissue involved in glucose uptake, and thus is important in organismal glucose metabolism. In C2C12 cells, gene expression of pyruvate dehydrogenase kinase 4 (PDK4), an important enzyme in the regulation of glucose consumption, was shown to be positively regulated by Foxo1, indicating the role of Foxo1 in regulation of energy metabolism (45). Interestingly, transgenic mice overexpressing Foxo1 specifically in skeletal muscle had impaired glycemic control after both oral glucose and intraperitoneal insulin injection (38).

Expression of Foxo1 and Foxo3 is upregulated in mouse gastrocnemius during 24 hour starvation. After 24 hours of refeeding, Foxo1 and Foxo3 gene expression returned to normal levels. During starvation, blood-glucocorticoid levels increased. In response to glucocorticoid treatment, Foxo1 expression increased three-fold and Foxo3 and Foxo4 increased slightly, as well. These results indicate that elevated glucocorticoids are sufficient to increase expression of Foxo transcription factors and may be directly

responsible for the increase in Foxo expression that results in skeletal muscle from starvation (45).

3. Age-dependent activity

Muscle atrophy is a major symptom of aging, and thus age-dependent activity of Foxo is of interest. The role of the Foxo transcription factors in aging was explored by Furuyama et al. They determined that Foxo3A and Foxo4 mRNA were elevated in the skeletal muscle of 6 month old rats in comparison to 3 and 26 month old rats; however no change in the Foxo1 mRNA levels with age was detected. They concluded that the caloric restriction-induced increase in Foxo1 and Foxo4 mRNA can decrease aging (52).

In the mouse diaphragm, DNA binding activity is regulated by both age and mechanical stimulation. Pardo et al. determined that DNA binding activity of Foxo1 and Foxo3A were significantly reduced in the diaphragms of 2-month old mice that had undergone constant mechanical stretch to 2.22 g/cm for 15 minutes compared to in the diaphragms of control mice which had not been stretched. However, this decrease in activity was not seen in the diaphragms of 24-month old mice after 15 minutes of constant mechanical stretch. Furthermore, basal DNA-binding activity of Foxo1 and Foxo3A were lower in the diaphragms of 24-month old mice than in those of 2 month old mice, demonstrating the age-sensitivity of Foxo1 and Foxo3A in the diaphragm (43).

Temporal regulation is seen not only in the diaphragm. Foxo1 is highly expressed in developing blood vessels. At E9.5, *Foxo1*-null mice vasculature showed immature development, indicating that Foxo1 plays an important role in embryonic angiogenesis,

but not in the initial vasculogenesis. The age-dependent reduced fertility of *Foxo3A*-null mice is another example of the importance of temporal regulation of Foxo (39).

4. Muscle Atrophy

Muscle atrophy is characterized by a decrease in overall muscle size due to a reduction in the size of individual fibers. Both Foxo1 and Foxo3A control the delicate balance between muscle atrophy and muscle hypertrophy. In transgenic mice overexpressing Foxo1 selectively in skeletal muscle, lower net body mass and smaller muscles were observed, demonstrating Foxo1 to be sufficient to induce muscle atrophy (38). Overexpression of Foxo3A, in both C2C12 myotubes and tibialis anterior fibers induced atrophy, whereas expression of dominant negative Foxo3A prevented muscle atrophy (19). Foxo1 has also been shown to mediate muscle atrophy in both DNA binding-dependent and binding–independent manners (53).

Two major pathways mediate the proteolysis which underlies muscle atrophy: the ubiquitin/proteasomal pathway and the autophagic/lysosomal pathway. In the ubiquitin/proteasomal pathway, proteins are tagged with ubiquitin and thus marked for subsequent proteasomal degradation (54). In the lysosomal pathway, portions of the cell are enclosed in vacuoles called autophagosomes. Autophagosomes fuse with lysosomes and degradation occurs via lysosomal hydrolases (55).

Two E3 ubiquitin ligases, atrogin-1 (MAFbx) and MuRF1, were determined to be necessary to Foxo regulation of muscle atrophy (56). E3 ubiquitin ligases are part of the ubiquitin/proteasomal pathway and catalyze the attachment of ubiquitin to proteins, thus marking them for degradation (57). Therefore, Foxo is often referred to as a part of the

ubiquitin/proteasomal pathway. However, increased expression of the lysosomal proteinase Cathepsin L in transgenic mice overexpressing Foxo1 selectively in skeletal muscle indicates that the cause for the decrease in size of muscle fibers is lysosomal protein degradation (38). Foxo3 has been shown to regulate the transcription of *LC3* and *Bnip3*, two autophagy genes, providing further evidence of the role of lysosomal degradation in Foxo-mediated atrophy. Foxo3 controls both the ubiquitin/proteasomal pathway and the autophagic/lysosomal pathway independently (25). Caspases (58) and calpains (59) may play a role in proteolysis leading to atrophy, as well. However, lysosomal and proteasomal degradation account for approximately 90% of proteolysis occurring in atrophying muscle, indicating that any effect that caspases and calpains have is minimal (60). While Foxo3 controls both the ubiquitin/proteasomal pathway and the autophagic/lysosomal pathway independently (25), lysosomal degradation accounts for the greater portion of proteolysis which occurs in Foxo3-induced muscle atrophy (60).

5. Excitation-contraction coupling

The method by which electrical stimulation of a muscle fiber is converted to muscle contraction is termed excitation-contraction (EC) coupling. This process includes the depolarization of the cell membrane, internal changes in the Dihydropyridine receptors (DHPRs) which are mechanically coupled with skeletal muscle Ryanodine receptor Ca^{2+} channels (RyR1), and induction of rapid Ca^{2+} release from the sarcoplasmic reticulum (SR) into the cytosol via RyR1 (61-63). Depolarization of the fiber causes an action potential which is propagated both radially and inwardly, primarily via charge movement through Nav1.4, the sodium channel skeletal muscle isoform, all along the sarcolemma and through the transverse (T-) tubule system of the fiber (64, 65).

G. Clinical implications

The Foxo pathway leads to activation of atrogenes such as atrogin-1 and MuRF-1 (19, 53, 56). Although the pathway for Foxo1 regulation has been explored in depth in many muscle and non-muscle tissue types, the extent and kinetics of its nuclear-cytoplasmic redistribution in response to various physiological, pathological, and pharmacological stimuli has not been fully defined in skeletal muscle, where the mechanism underlying muscle atrophy is of therapeutic interest. Many kinases which are active in the phosphorylation of Foxo1 have been identified in different cell types, but their location and nuclear or cytoplasmic activity have not been investigated in muscle or other cell types. Further characterization of this pathway may help in the development of new therapeutic avenues to minimize, and possibly treat, skeletal muscle atrophy in diseases such as sepsis, severe insulinopenia, HIV, and particularly age-related muscle atrophy.

CHAPTER 2

KINETICS OF NUCLEAR-CYTOPLASMIC TRANSLOCATION OF FOXO1 AND FOXO3A IN ADULT SKELETAL MUSCLE FIBERS

The information contained in this chapter was published in American Journal of Physiology- Cell Physiology. As first author, I carried out the experiments and their analysis. Together with Drs Tiansheng Shen and Martin Schneider, the experiments were planned and interpreted.

A. INTRODUCTION

The Fox (forkhead box) transcription factor superfamily, including the Foxo family, is characterized by a common 100-residue DNA-binding domain known as the forkhead domain. Foxo is an evolutionarily conserved transcription factor family that is a major

player in many vital cellular functions such as cell proliferation, cell cycle, and cellular survival (6, 46). There are 4 members of the forkhead transcription factor family in humans; Foxo1, Foxo3A, Foxo4, and Foxo6. These are all expressed in skeletal muscle except Foxo6 which is mainly expressed in the brain (37). In adult mice, Foxo1 is expressed in many tissue types but most strongly in ovary and uterus tissue, Foxo3 (the murine ortholog of Foxo3A) is expressed in all tissue types studied in Biggs et al., 2001, whereas Foxo4 is only expressed in skeletal muscle (5). However, Foxo1 and Foxo3A are the forkhead transcription factors associated with muscle atrophy and upregulation of either one individually has been shown to be sufficient to induce muscle atrophy (19, 38). Foxo1 knockout mice are embryonic lethal and cre-mediated disruption of Foxo1 expression indicates that Foxo1 acts as a tumor suppressor (39, 48). In muscle, Foxo1 has been shown to regulate myotube differentiation and skeletal muscle fiber type remodeling (24, 47). Activation of the Foxo pathway leads to expression of atrogene products atrogin-1/MAFbx and MuRF-1, proteins that are integral to the development of muscle atrophy (19, 53, 56).

The phosphorylation status of Foxo regulates its nuclear entry and activation of atrogenes. Foxo1 has three highly conserved Akt (also known as protein kinase B, PKB) phosphorylation sites; Thr-24, Ser-256, and Ser-319; in human Foxo1 (6-8). Many growth stimuli, such as insulin-like growth factor- (IGF) 1, can bind to membrane-bound receptors which activate phosphatidylinositol-3-kinase (PI3K) and subsequently Akt (21, 22). Although the primary regulation of Foxo occurs through Akt-mediated phosphorylation, serum- and glucocorticoid-inducible kinase (SGK) has the ability to phosphorylate these residues as well. Casein kinase 1 (CK1), DYRK1A, and other

kinases have different recognized phosphorylation sites (10-12). Ser-256, which is phosphorylated by Akt, is located in a basic region at the C-terminal end of the DNA binding domain (DBD) that has been shown to function as a nuclear localization signal (NLS; reference 15). There is a leucine-rich nuclear export signal (NES) in the region C-terminal to the DBD of Foxo1. In FL5.12 and NIH 3T3 cell lines, phosphorylated Foxo1 can be dephoshosphorylated by PP2A, a serine/threonine phosphatase, allowing Foxo1 to enter the nucleus. Okadaic acid (OA), a PP2A inhibitor, prevents this dephosphorylation, thereby inhibiting the nuclear influx of Foxo1 (14).

Although the pathway for Foxo1 regulation has been explored in depth in many muscle and non-muscle tissue types, the extent and kinetics of its nuclear-cytoplasmic redistribution in response to various physiological, pathological, and pharmacological stimuli has not been fully defined in skeletal muscle, where the mechanism underlying muscle atrophy is of therapeutic interest. Further characterization of this pathway strives to aid in the development of new therapeutic avenues to minimize, and possibly treat, skeletal muscle atrophy in diseases such as sepsis, severe insulinopenia, HIV, as well as age-related muscle atrophy (14).

Here, we use confocal microscopy to image adenovirally expressed Foxo1-GFP (adFoxo1-GFP) or Foxo3A-GFP (adFoxo3A-GFP) in living cultured adult skeletal muscle fibers to determine the kinetics of their nuclear-cytoplasmic translocation and what factors affect theses kinetics. We demonstrate that under resting conditions Foxo1 is cycling into and out of the nucleus rapidly, but Foxo3A is cycling 20 times slower. Nuclear entry of Foxo1 can be blocked by activation of the IGF-1/PI3K/Akt pathway or by inhibition of the phosphatase PP2A. Leptomycin B (LMB) irreversibly binds to

chromosome region maintenance 1 (CRM1) and inhibits nuclear efflux of Foxo1, thereby enabling the calculation of the rates of unidirectional nuclear influx under conditions with different levels of phosphorylation of Foxo1. Comparison of the responses of endogenous Foxo1 and adenovirally expressed Foxo1-GFP to the treatments described above identifies our model system as being an accurate and useful tool in the kinetic study of changes in subcellular distribution of Foxo1 in skeletal muscle fibers.

B. METHODS

1. Materials

Okadaic acid, staurosporine, and IGF-1 were purchased from Sigma Aldrich (St. Louis, MO) and Leptomycin B from LC Laboratories (Woburn, MA). The Akt inhibitor Akt-I-1,2 and the PI3K inhibitor LY294002 were obtained from Calbiochem (Darmstadt, Germany).

2. Isolation and culture of adult FDB muscle fibers

The flexor digitorum brevis (FDB) was isolated from adult female CD1 mice (4-6 weeks old). Animals were euthanized by asphyxiation via CO_2 followed by cervical dislocation according to protocols approved by the University of Maryland Institutional Animal Care and Use Committee. Individual fibers were enzymatically dissociated and cultured using a modified protocol previously described in Liu et al, 2009 (66). Briefly, the muscle was incubated in MEM (Invitrogen, Carlsbad, CA) containing 3.5 µg/ml Collagenase type I (Sigma-Aldrich), 10% FBS, and 50 µg/ml gentamicin for 2 hours at 37˚ to enzymatically

dissociate the muscle. Manual manipulation to separate individual fibers was done by triturating the muscle gently in media containing no collagenase. Approximately 50 fibers were then plated in a laminin-coated glass-bottomed dish.

3. Adenoviral infection of cultured FDB fibers

Fibers were plated in 2 ml serum-free MEM with 9.2 x 10^4 PFU/µl adFoxo1-GFP or 4.8 x 10^3 PFU/µl adFoxo3A-GFP lysate and incubated for 48-72 hours. The adenovirus encoding Foxo1-GFP was a gift from Dr. Joseph Hill (University of Texas Southwestern Medical Center, reference 67) and the Foxo3A-GFP adenovirus was purchased from Applied Biological Materials (Richmond, British Columbia, Canada; catalog #000420A). Both adenoviruses were amplified in our lab. In both constructs, the GFP fusion tag is attached at the C-terminal of Foxo.

4. Confocal fluorescence imaging of living cultured adult muscle fibers

Half hour prior to imaging, the culture dish was removed from the incubator and the culture media was removed and replaced with L-15 media (Invitrogen). The culture dish was then set on the stage of an Olympus IX70 inverted microscope equipped with an Olympus FLUOVIEW 500 laser scanning confocal imaging system, with excitation wave-lengths of 488 nm and 647 nm. Fibers were viewed with an Olympus 60X/1.2 NA water-immersion objective and scanned at zoom 3 (except Figures 2.1A-B and 2.3A-B which were scanned at zoom 1) using consistent laser output and gain. Then, 30 minutes after media change to L-15, images were taken for 30 minutes at 10 minute increments to establish a stable baseline in each individual fiber. After the last baseline image was taken, LMB or other treatment was added to the dish and time was set to begin from 0

minutes at that point. Once the experiment began, the medium was not removed at any point; only additions of small volumes of reagents were made.

In cases of strong nuclear uptake of Foxo1-GFP, including the fiber in **Figure 2.3B**, the nuclei of the fiber reached saturation of our detection system using the control laser intensity. Therefore, continued imaging used decreased laser intensity to avoid nuclear saturation. However, the images shown in **Figure 2.3** were taken at the original laser intensity with saturated nuclei for qualitative comparison to show the overall extent of the effect. The change in laser intensity when saturation occurs does not affect our quantification of nuclear concentration because we calculate the nuclear concentration as a nuclear to cytoplasmic fluorescence ratio, and both the nuclear and cytoplasmic fluorescence are affected by the same percent by change in laser intensity.

5. Image analysis

The mean pixel fluorescence of the cytoplasm and nucleus from each image was quantified using an area of interest in Image J as indicated in **Figures 2.3A and 2.3C**, and then the background mean pixel fluorescence was subtracted from each. The ratio of nuclear mean pixel fluorescence to cytoplasmic mean pixel fluorescence (n/c) is calculated for each time point to allow comparison of nuclear fluorescence independent of expression levels of Foxo1-GFP and should be proportionate to nuclear concentration normalized to cytoplasmic level of expression. Student's t-tests were used for comparisons of data obtained from two experimental conditions, and differences were considered significant if $p < 0.05$.

6. Fluorescence immunocytochemistry

Fluorescence immunocytochemistry was carried out as in Shen et al. (68). Briefly, fibers were fixed with 4% paraformaldehyde, permeabilized with 0.2% Triton-X-100 in PBS, and then blocked with 5% normal goat serum. Fibers were incubated with anti-Foxo1 (Cell Signaling, #2880), anti-α-actinin (Sigma), or anti-nucleophosmin (Zymed, San Francisco, CA) overnight followed by overnight incubation with a fluorescent-tagged secondary antibody. The stained fibers were imaged using the confocal microscope and lasers described above. Colocalization of immunofluorescence images were merged, mean pixel fluorescence measured as a function of distance for tracings, and enhanced using Image J. No other image in this paper was enhanced.

7. Western blotting

Protein extraction and western blotting techniques were performed as described in Shen et al. (69). Briefly, FDB were cultured for 2 days and then treated for 80 minutes as indicated. Fibers were then collected and mixed with M-PER (Thermo Scientific, Rockford, IL) and a protease inhibitor cocktail (Roche Diagnostics, Indianapolis, IN) and passed through a 21 gauge syringe several times, followed by high speed centrifugation. The supernatant was combined with sample reducing agent and LDS sample buffer (Invitrogen), heated at 70° for 10 min, and run on a NuPAGE Novex 4-12% Bis- Tris gel (Invitrogen). Proteins were transferred to a PVDF membrane. Akt antibody (Cell Signaling, #9271) and phosphospecific Akt antibody (Cell Signaling, #9271) were used and the membrane was then treated with ECL and film was exposed and developed.

C. RESULTS

1. Adenovirally expressed Foxo1-GFP is distributed in a manner consistent with endogenous Foxo1 in adult muscle fibers

To establish a live adult muscle fiber system to explore the phosphorylation dependency of the kinetics of Foxo1 nuclear-cytoplasmic translocation in skeletal muscle, we infected cultured adult FDB fibers with an adenovirus coding for Foxo1-GFP, which can be tracked quantitatively in subcellular regions of living muscle fibers using fluorescence confocal microscopy. To validate this system, we first compared the sarcomeric localization as well as nuclear-cytoplasmic distribution of endogenous Foxo1 to that of adenovirally expressed Foxo1-GFP (**Figure 2.1**). Using immunocytochemistry we established the subsarcomeric colocalization of endogenous Foxo1 with α-actinin (**Figure 2.1A, right panel**), a well-established Z-line protein. Foxo1-GFP also colocalized with α-actinin (**Figure 2.1B, right panel**), demonstrating consistent Z-line localization of both expressed Foxo1-GFP and endogenous Foxo1. In agreement with these findings, antibody staining of Foxo1 and the fluorescence of Foxo1-GFP in fibers expressing Foxo1-GFP displayed colocalization (data not shown). Under resting conditions, Foxo1-GFP is also present in the nuclei in a generally diffuse pattern (**Figure 2.1B, left panel**), but does not enter the nucleolus (data not shown).

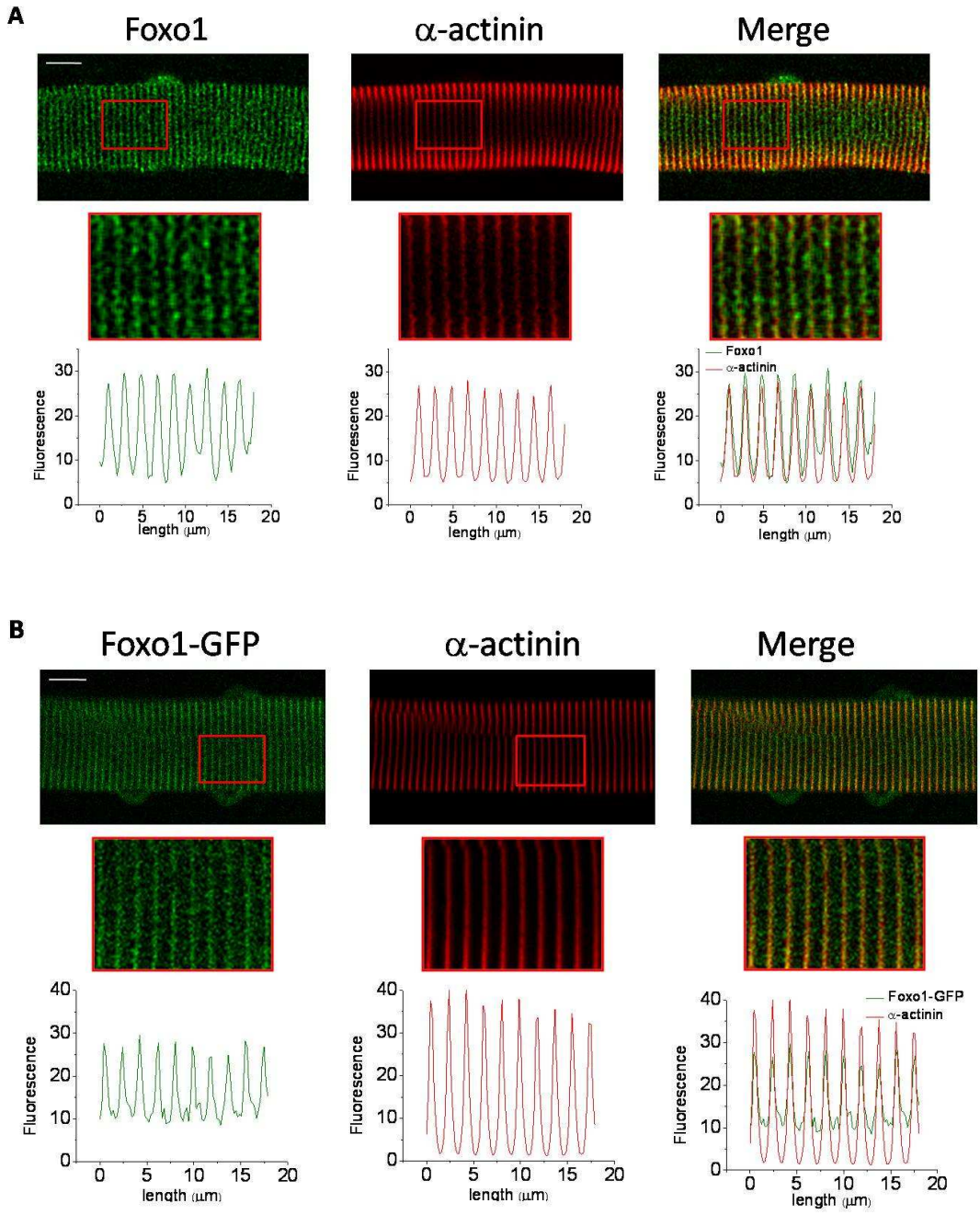

Figure 2.1 Subsarcomeric distribution of endogenous Foxo1 and exogenous Foxo1-GFP.

Representative confocal images of immunocytochemistry assays of endogenous Foxo1 (**A**) and fluorescence of Foxo1-GFP (**B**) with α-actinin establish its Z-line localization. Each top figure shows a large section of a fiber with a red square indicating the segment of the fiber that is magnified below it. Below each enlarged region is a graph demonstrating the total fluorescence of the enlarged region as a function of distance as detailed on the x-axis. Scale bars are 10 μm.

We next compared the nuclear/cytoplasmic mean pixel fluorescence (n/c) ratios of immuno-stained Foxo1-GFP and endogenous Foxo1 under control conditions. The normalization to cytoplasmic levels provides a means of comparing the concentrations of nuclear Foxo1 in a manner that is not expression-dependent. The n/c ratios attained using immunocytochemistry of endogenous Foxo1 agreed very closely with n/c ratios of immuno-stained Foxo1-GFP under control conditions (**Figure 2.2A**).

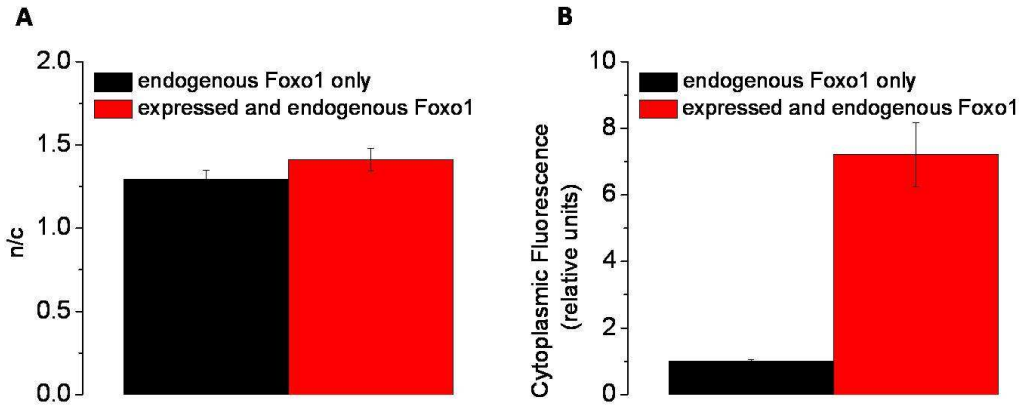

Figure 2.2 Nuclear/cytoplasmic fluorescence ratios of expressed Foxo1-GFP and endogenous Foxo1.

(A) Quantification of nuclear/cytoplasmic fluorescence ratios (n/c) of Foxo1-GFP (n=16/20) in black and antibody stain for endogenous Foxo1 (n=16/22) in red showing nuclear/cytoplasmic distribution to be comparable under control conditions as determined using immunocytochemistry. (B) Foxo1-GFP (n=20) is determined to be expressed at a level 7-fold that of endogenous Foxo1 (n=22). Data are represented as means ± SE.

To further characterize our conditions, we compared the cytoplasmic anti-Foxo1 fluorescence levels in fibers expressing Foxo1-GFP and in non-infected control fibers. We treated both sets of fibers with anti-Foxo1 primary antibody and conjugated Alexa-

647 secondary antibody (which does not interfere with GFP emissions) and found that the total Foxo1 cytoplasmic concentration in infected fibers was approximately 7-fold that of uninfected fibers (**Figure 2.2B**). A typical area of interest used for determining the mean pixel fluorescence of the cytoplasm in a confocal image for a given fiber is shown in red in the left image in **Figure 2.3A** and that for a nucleus is shown in red in **Figure 2.3C**.

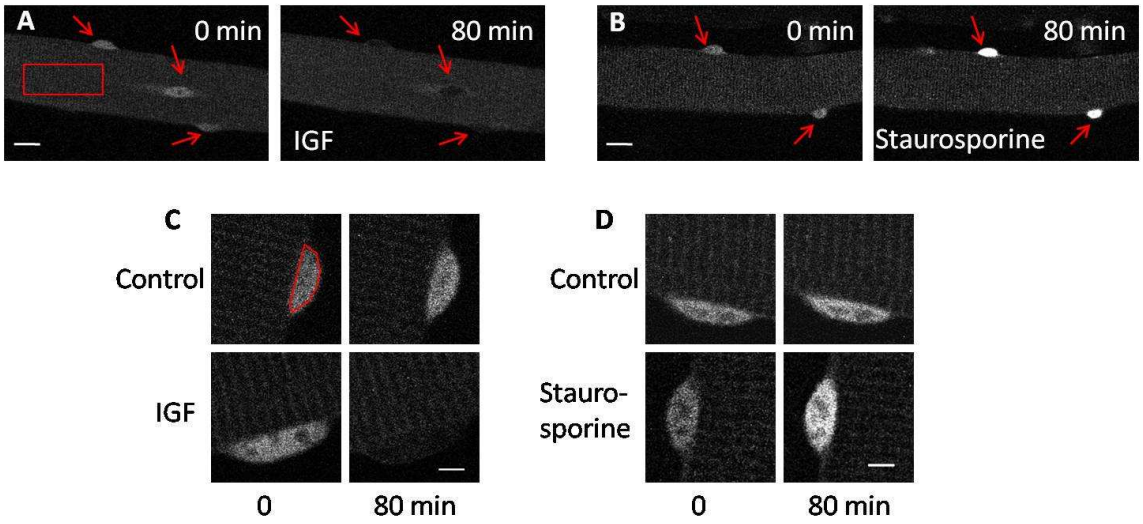

Figure 2.3 Broad spectrum kinase inhibitor staurosporine promotes Foxo1 nuclear entry.

Representative confocal images of single fibers at 0 and 80 minutes of IGF-1 (**A**) or staurosporine (**B**) treatments, as labeled. Red arrows point to nuclei. Over 80 minutes of IGF-1 treatment the nuclear concentration of Foxo1 nuclei decreases visibly whereas the nuclei of the fiber treated with staurosporine increase to the point of saturation. The red box indicates an average cytoplasmic region used to quantify cytoplasmic fluorescence. Scale bars are 20 μm. Magnification of individual nuclei from control fibers, a fiber treated with IGF-1 (**C**), and a fiber treated with staurosporine (**D**), as labeled. The fluorescence of the control nuclei increase very slightly whereas IGF-1 treatment causes a decrease in nuclear fluorescence and staurosporine treatment causes an increase in nuclear fluorescence. The red outline in panel C indicates the nuclear region used to quantify nuclear fluorescence. Scale bars are 5 μm.

The similarity in sarcomeric localization and nuclear-cytoplasmic distribution of expressed Foxo1-GFP and endogenous Foxo1, coupled with consistency in response to phosphorylating and dephosphorylating agents (see **Figure 2.4**, below) leads us to conclude that adenovirally expressed Foxo1-GFP is a good model for endogenous Foxo1. The system of adenovirally expressed Foxo1-GFP in cultured adult skeletal muscle fibers is thus a useful tool for real-time monitoring of kinetics of translocation of Foxo1 in live cells in a quantitative manner.

2. Nuclear-cytoplasmic movements of Foxo1 are kinase-dependent

Under the standard conditions used for these studies, fibers exposed to adenovirus Foxo1-GFP were cultured in serum-free media without added growth factors for 48 to 72 hours. The media was then changed to L-15 imaging media (as described in the *materials and methods* section above) with no added growth factors or serum. Treatment with 100 ng/ml IGF-1, a concentration that produces both mytogenic and myogenic responses in cultured myoblasts (70), caused a rapid and marked reduction in the concentration of nuclear Foxo1-GFP (**Figures 2.3A and C**). After 20 minutes of IGF-1 treatment, nuclear/cytoplasmic Foxo1-GFP decreased to 20% of control, and by 40 minutes reached a steady level of 10% of control (**Figure 2.4A, red line**). In comparison, a gradual increase in nuclear/cytoplasmic fluorescence of Foxo1-GFP was observed over the same time period in control fibers where no changes were made to the medium bathing the fibers (**Figures 2.4A-D, black line**). This slow increase in nuclear/cytoplasmic Foxo1-GFP fluorescence is likely due to the previous removal of the culture media, which presumably contained secreted autocrine/paracrine growth factors produced by fibers during the 48-72 hours of fiber culture (71), and the subsequent

addition of growth factor-free imaging media. The cytoplasmic fluorescence showed little change with time when IGF-1 was included in the imaging media (data not shown).

Figure 2.4 IGF-1 promotes reduction of nuclear Foxo1, whereas staurosporine and inhibitors of PI3K and Akt increase nuclear Foxo1.

(**A**) 100 ng/ml IGF-1 treatment causes a decrease in nuclear/cytoplasmic fluorescence ratio (n/c) of Foxo1 (n=4) over time in comparison to control fibers (n=4). (**B**) Treatment with 1 μM staurosporine (n=4) causes an increase in n/c Foxo1 above control levels (n=5) indicating kinase-dependency of Foxo1 cytoplasmic retention. Inhibition of PI3K (**C**) via LY294002 (n=4; control n=4) or inhibition of Akt (**D**) by Akt-I-1,2 (n=4; control n=7) increases the concentration of nuclear Foxo1. This indicates that the activity of PI3K and Akt are individually necessary for cytoplasmic retention of Foxo1. (**E**) Treatment with staurosporine (stauro), LY294002, and Akt-I-1,2 inhibited phosphorylation of Akt whereas IGF treatment increased phosphorylation of Akt as demonstrated with western blotting techniques for Akt and Akt phosphorylated at S473. Bar graphs of relative increase of nuclear Foxo1 as a fraction of control conditions in Foxo1-GFP (**F**) and endogenous Foxo1 (**G**) after 80 minutes control (endogenous n=26; Foxo1-GFP n=19) or 80 minutes treatments with IGF-1 (endogenous n=27; Foxo1-GFP n=4), staurosporine (endogenous n=23; Foxo1-GFP n=3), or Akt-I-1,2 (endogenous n=29; Foxo1-GFP n=6) as labeled. Autofluorescence and background values were subtracted from endogenous nuclear and cytoplasmic fluorescence values. Data are represented as means ± SE.

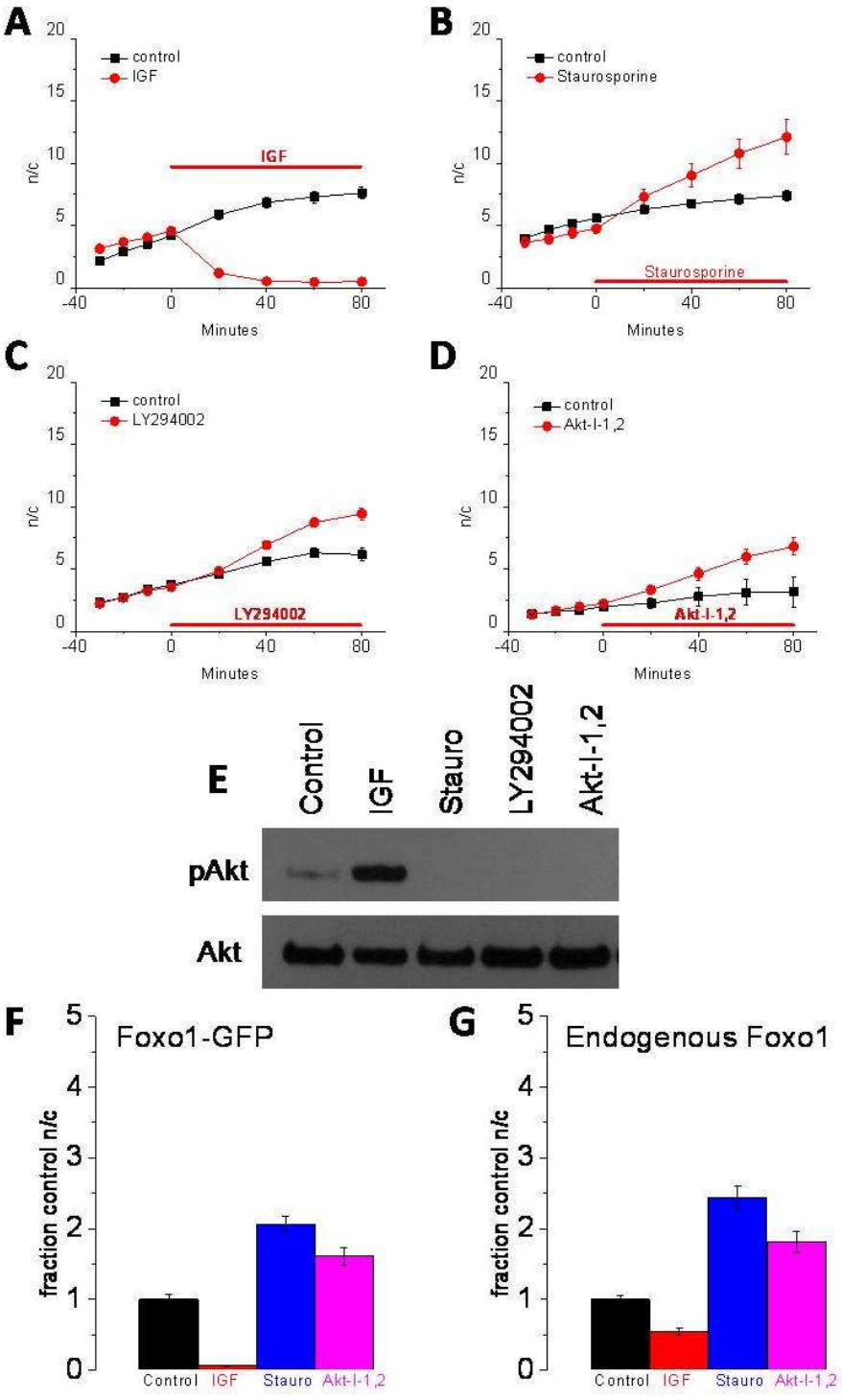
A
control
IGF
IGF
n/c
Minutes
B
control
Staurosporine
Staurosporine
n/c
Minutes
C
control
LY294002
LY294002
n/c
Minutes
D
control
Akt-I-1,2
Akt-I-1,2
n/c
Minutes
E
Control
IGF
Stauro
LY294002
Akt-I-1,2
pAkt
Akt
F
Foxo1-GFP
fraction control n/c
Control
IGF
Stauro
Akt-I-1,2
G
Endogenous Foxo1
fraction control n/c
Control
IGF
Stauro
Akt-I-1,2

Treatment with 1 μM staurosporine, a non-specific kinase inhibitor, had the opposite effect from IGF-1; it caused a rapid increase in nuclear Foxo1 (**Figures 2.3B, 2.3D, and 2.4B**). After 20 minutes, the nuclear concentration of Foxo1 increased by 40%, and over 80 minutes it increased by 144% (**Figure 2.4B**). The opposite changes in nuclear Foxo1-GFP in response to treatment with IGF-1, an upstream activator of several kinases including Akt, and staurosporine, a non-specific kinase inhibitor, demonstrate the phosphorylation dependence of nuclear fluxes of Foxo1.

3. PI3K/Akt pathway is necessary for Foxo1 phosphorylation

In order to determine the pathway(s) involved in the phosphorylation of Foxo1, which regulates the nuclear cytoplasmic fluxes of Foxo1, we employed specific kinase inhibitors. 25 μM LY294002, a specific PI3K inhibitor, induced an increase in nuclear Foxo1-GFP within 40 minutes (**Figure 2.4C**). Akt-I-1,2 is a selective inhibitor of Akt 1 and Akt 2 that does not cause significant inhibition of other kinases with the exception of CaMK1, a kinase which, to our knowledge, does not affect the phosphorylation status of Foxo1 (72, 73). 1 μM Akt inhibitor, Akt-I-1,2 (**Figure 2.4D**), also caused an increase in nuclear Foxo1-GFP. As determined by western blot and a phospho-specific Akt antibody, 80 minutes of treatment with staurosporine, LY294002, or Akt-I-1,2 each efficiently inhibited phosphorylation of Akt (**Figure 2.4E**). These data indicate that the PI3K/Akt pathway is necessary to block Foxo1 nuclear entry.

We also compared the relative values of n/c ratios obtained for Foxo1-GFP and for endogenous Foxo1 under control conditions to n/c ratios in the presence of phosphorylating agents and phosphorylation inhibitors, and determined that the ratios are

similar under the same condition, further validating the use of exogenous Foxo1-GFP to monitor Foxo1 movement in living fibers (**Figures 2.4F-G**).

4. Inhibition of PP2A via Okadaic acid decreases nuclear Foxo1

The phosphatase PP2A has been shown to directly dephosphorylate Foxo1 in the FL5.12 cell line expressing doxycycline-inducible wild type Foxo1 (14). Treatment of cultured muscle fibers with 100 nM okadiac acid (OA), a selective inhibitor of the PP2A class of phosphatases at this concentration (74), drastically reduced nuclear Foxo1 and inhibited the increase in nuclear Foxo1 that occurs with time in control fibers (**Figure 2.5A-B**), implicating PP2A as a Foxo1 phosphatase in skeletal muscle.

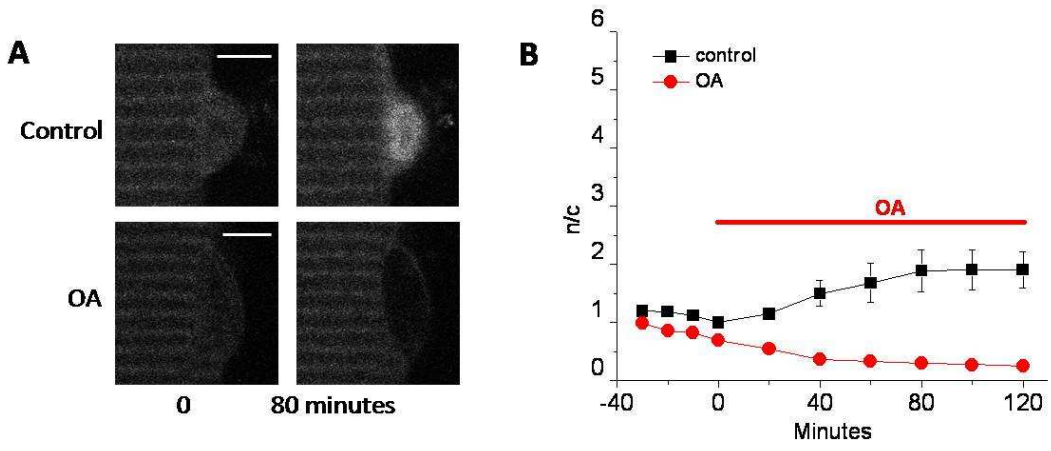

Figure 2.5 PP2A inhibitor okadaic acid reduces Foxo1-GFP nuclear influx.

(**A**) Representative confocal images of two fibers at 0 and 80 minutes of 100 nM OA treatment (bottom panels) or under control conditions (top panels). Scale bars are 5 μm. (**B**) Quantification of nuclear/cytoplasmic fluorescence ratio (n/c) Foxo1-GFP versus time during 100 nM OA (n=5) or control (n=4) treatment demonstrates OA ability to decrease nuclear Foxo1. Data are represented as means ± SE.

5. Nuclear-cytoplasmic shuttling of Foxo1

The results presented thus far show changes in net nuclear Foxo1 resulting from differences between nuclear influx and efflux of Foxo1. However, the magnitudes of the simultaneously occurring nuclear efflux and influx underlying the observed net flux was not determined. Treatment with a maximally effective concentration of LMB, an irreversible inhibitor of the export carrier CRM1, should eliminate nuclear export of Foxo1. Under this condition, the time course of the resulting buildup of nuclear Foxo1 would then occur at a rate equal to its rate of unidirectional flux out of the cytoplasm and into the nucleus. Therefore, using LMB we can calculate the rate of nuclear influx of Foxo1 under various conditions. Under resting conditions, nuclear influx of Foxo1-GFP occurs at a fast pace in LMB - during 80 minutes of exposure to 40 nM LMB, nuclear Foxo1 increased 10 fold (**Figures 2.6 A-B**). Because there is no substantial buildup of Foxo1 without LMB under the same (control) conditions, we conclude that fast shuttling of Foxo1 into and out of the nucleus occurs in the absence of LMB. 20, 40, and 80 nM LMB induced the same rate of nuclear buildup of Foxo1, indicating that CRM-1 is maximally inhibited by 40 nM LMB under these conditions (**Figure 2.6C**).

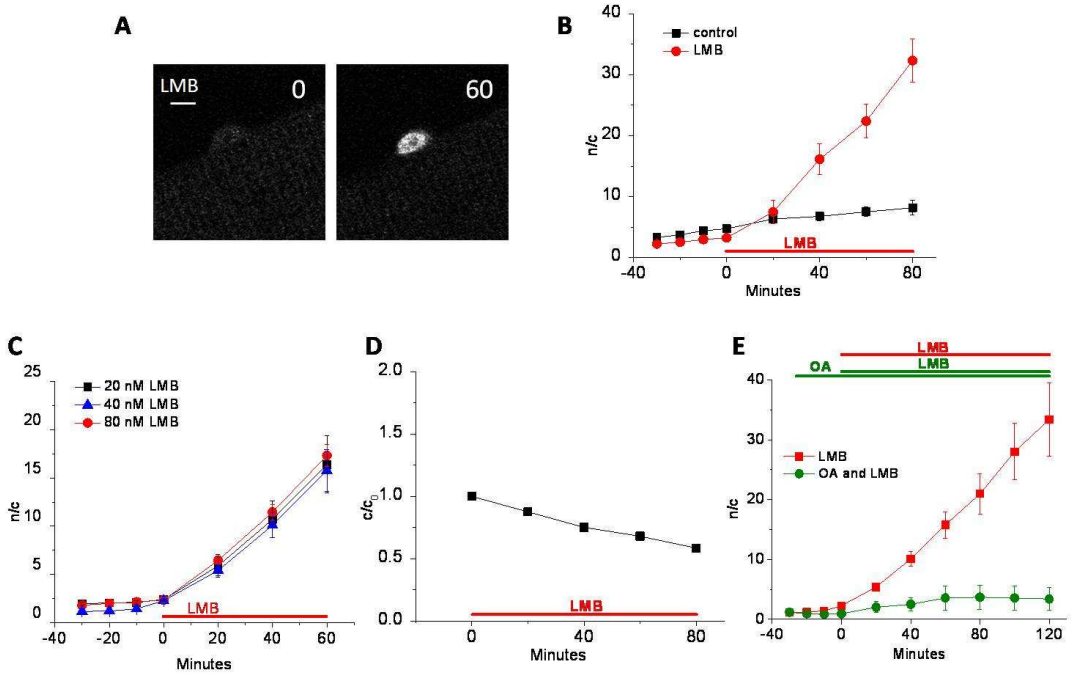

Figure 2.6 Leptomycin B eliminates nuclear efflux of Foxo1 and allows direct measurement of the unidirectional rate of nuclear influx of Foxo1.

(**A**) Representative confocal images of a single muscle fiber treated with 40 nM LMB for the time indicated. Nuclear Foxo1 increases with LMB treatment. Due to saturation, laser intensity was decreased for the second image. Nuclear/cytoplasmic fluorescence (n/c) ratio is used to measure nuclear Foxo1 in an expression independent manner and to normalize for the change in laser intensity. Scale bar is 5 μm. (**B**) Quantification of the increase in nuclear Foxo1 in control (n=5) and LMB-treated (n=5) fibers. (**C**) Time course of the effects of 20 (n=7), 40 (n=5), and 80 (n=7) nM LMB treatment on Foxo1 n/c. (**D**) As the nuclear concentration of Foxo1 increases with LMB treatment the cytoplasmic concentration decreases (n=12). (**E**) Addition of 100 nM OA in tandem with 40 nM LMB (n=3) prevents the buildup of nuclear Foxo1 in comparison to that seen in LMB-treated fibers (n=5). Data represented as means ± SE.

In contrast to our studies without LMB, where Foxo1-GFP is not strongly accumulated in the muscle fiber nuclei, during LMB treatment Foxo1-GFP can become highly concentrated in the nuclei and the cytoplasmic Foxo1-GFP fluorescence visibly decreases. Over 80 minutes of LMB treatment, the cytoplasmic fluorescence is reduced

by about half (**Figure 2.6D**), whereas in control conditions without LMB treatment, the cytoplasmic fluorescence does not change noticeably (data not shown).

By conservation of mass,

$$\Delta c\ V_c = -\Delta n\ V_n\ , \qquad (1)$$

where Δc and Δn are the coreresponding changes in c and n when a given amount of Foxo1-GFP moves between the cytoplasm and the nuclei of a muscle fiber and V_c and V_n are the cytoplasmic and nuclear volumes. The mean value of $-\Delta c/\Delta n$ obtained from 11 fibers exposed to LMB for 80 minutes was 0.05 +/- 0.001, which equals the mean value of V_n/V_c in these muscle fibers.

6. Role of cytoplasmic phosphatase

The PP2A inhibitor OA induces a decrease in nuclear Foxo1 in the absence of LMB (**Figures 2.5A-B**). To determine the manner in which this nuclear decrease occurs, fibers were or were not pretreated with OA for 30 minutes, followed by the addition of LMB. Using LMB to determine the rate of nuclear import of Foxo1, we established that OA effectively inhibits nuclear influx of Foxo1 (**Figure 2.6E**). During 60 minutes of OA and LMB treatment, the nuclear concentration of Foxo1 increased linearly with a slope of 0.04 n/c per minute in comparison to control fibers treated with only LMB, where the slope was 0.19 n/c per minute (**Figure 2.6E**). After 60 minutes of OA and LMB treatment, nuclear Foxo1 became constant. In contrast, in fibers treated with LMB alone, n/c continued to increase linearly during 60 minutes of LMB exposure, and showed a more than 10 fold increase over that of the nuclear concentration at 0 minutes, the point of addition of LMB (**Figure 2.6E**). Based on these data, we conclude that Foxo1 nuclear

import is induced by cytoplasmic dephosphorylation of Foxo1 via an OA-sensitive phosphatase, presumably PP2A.

7. Near balance between relatively large nuclear influx and nuclear efflux under resting conditions

In previous studies from our own and other laboratories, the observation of a rapid net nuclear influx during application of the CRM1-dependent nuclear efflux blocker LMB has been taken as evidence for the presence of relatively large, but near balanced nuclear influx and efflux prior to the addition of LMB (6, 46, 75). However, we are unaware of any previous reports of direct comparison of unidirectional influx and efflux rates under conditions of such nuclear-cytoplasmic shuttling of any molecule in any cell type. We therefore carried out experiments to directly address this point using our muscle fiber culture system. In order to improve time resolution, in these studies we used more frequent image acquisition, now at 2 minute intervals, compared to the preceding results which were based on images acquired at 10 or 20 minute intervals. We first monitored fibers under control conditions, and then added either a maximally blocking concentration of LMB (**Figure 2.7, red line**) or a highly effective concentration of IGF-1 (**Figure 2.7, black line**). The increase in nuclear Foxo1-GFP due to LMB addition begins with little delay, as expected for a direct, diffusion-limited pharmacological block of the nuclear export system by LMB. Subsequently, the nuclear accumulation of Foxo1 continues at a constant rate for the 40 minute recording interval after LMB addition. In contrast, the decrease in nuclear Foxo1-GFP on addition of IGF-1 begins with a clear time lag. This is as expected for the occurrence of a multi step signaling cascade initiated by IGF-1, but accomplished by the sequential activation of IGFR, PI3K and Akt, leading

to the eventual phosphorylation of Foxo1, which eliminates Foxo1 nuclear influx and promotes Foxo1 net nuclear efflux.

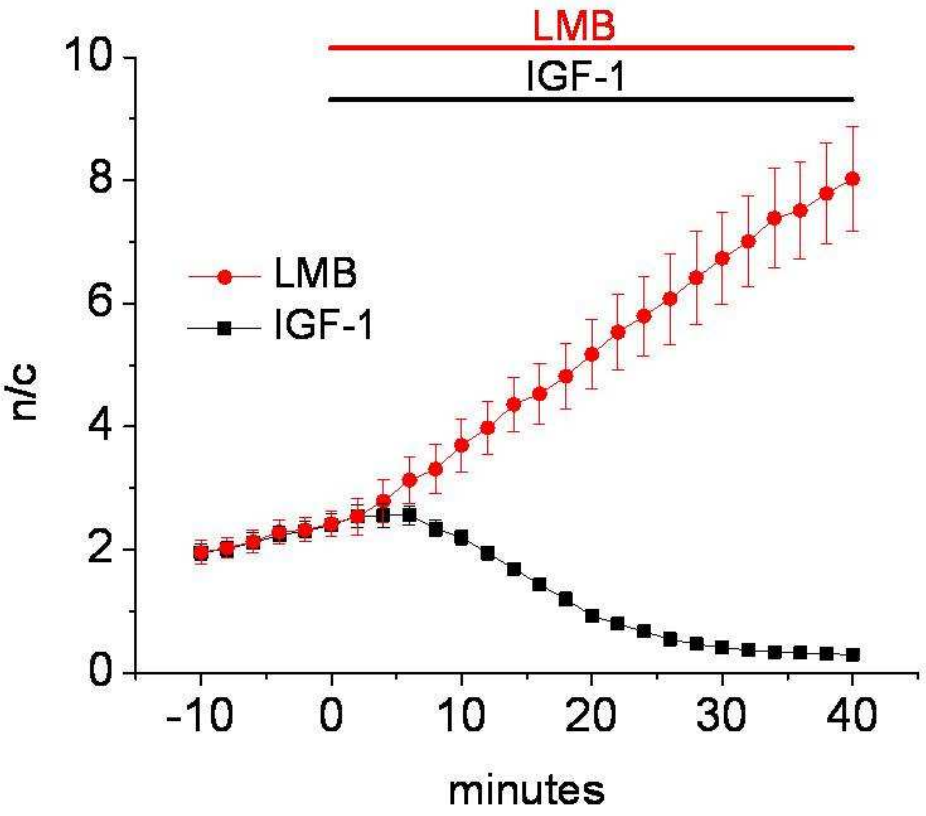

Figure 2.7 Nuclear-cytoplasmic shuttling of Foxo1-GFP.

After 10 minutes of imaging at 2 minute increments to attain a baseline value of the nuclear/cytoplasmic ration (n/c), fibers were treated with either 100 ng/ml IGF-1 (black line; n=5 nuclei from 4 fibers) or 40 nM LMB (red line; n=5 nuclei from 4 fibers) to prevent nuclear influx or efflux, respectively. The unidirectional rates of nuclear influx (0.16 +/- 0.03 n/c per min) and efflux (0.12 +/- 0.03 n/c per min) were calculated as the linear slope from 10 to 20 minutes of treatment.

In order to obtain a rough measure of the unidirectional flux rates under control conditions in **Figure 2.7** we used the mean flux rate from 10 to 20 min after reagent

addition. This gives a unidirectional influx rate of 0.16 +/- 0.03 n/c per minute (mean +/- SE) in 9 nuclei from 8 fibers from 2 experiments as in **Figure 2.7** in the presence of LMB, and a unidirectional efflux rate of 0.12 +/- 0.03 n/c per minute in 10 nuclei from 8 fibers in 2 other experiments in the presence of IGF-1. Assuming these unidirectional flux rates to apply to the control period prior to drug addition, the influx rate slightly exceeds the efflux rate, and would predict a relatively slow but systematic net influx of Foxo1 at a rate of 0.04 n/c per minute under control conditions prior to drug addition in **Figure 2.7**. This predicted value of net nuclear influx agrees very closely with the experimentally measured slopes of 0.04 +/- 0.01 and 0.03 +/- 0.02 n/c per minute obtained prior to addition of LMB or IGF-1, respectively.

8. Nuclear cytoplasmic shuttling is much slower for Foxo3A than for Foxo1

In a few experiments we examined the nuclear-cytoplasmic distribution and shuttling of Foxo3A in comparison to Foxo1. Under control conditions, the addition of LMB causes the nuclear fluorescence due to Foxo3A to continuously increase with time, indicating a constant rate of Foxo3A-GFP unidirectional nuclear influx. The rate of nuclear influx of Foxo3A in LMB then approximately doubled with the inhibition of Akt (**Figure 2.8A**). However, the rates of influx of Foxo3A in LMB are only approximately 1/20 of those of Foxo1, as seen by comparison of fibers from the same mouse infected with adenovirus for either Foxo1 or Foxo3A (**Figure 2.8B**). Note that the vertical scale in **Figure 2.8A** is compressed by a factor of 20 compared to that in **Figure 2.8B**, and that the same data points for Foxo3A-GFP are presented in **Figures 2.8A and B**. The mean values of the rate of increase of Foxo3A-GFP n/c were 0.0011 +/- 0.0005 n/c per min in control, 0.0073 +/- 0.0013 n/c per min in LMB and 0.014 +/- 0.003 n/c per min in LMB plus Akt-

I-1,2, and for Foxo1-GFP were 0.029 +/- 0.004 n/c per min in control, 0.16 +/- 0.018 n/c per min in LMB and 0.38 +/- 0.057 n/c per min in LMB plus Akt-I-1,2. Representative images of a single fiber in **Figure 2.8C** demonstrate the increase in nuclear Foxo3A during 80 minutes of LMB treatment and during an additional 60 minutes of Akt inhibition with continued LMB treatment.

Figure 2.8 Foxo3A cycling and phosphorylation by Akt.

(**A-B**) Foxo3A-GFP (red line; n=5 nuclei from 4 fibers) enters the nucleus at a slower rate than does Foxo1-GFP (black line in figure **B**; n=4), as determined using Leptomycin B (LMB) to inhibit nuclear efflux. Inhibition of Akt via Akt-I-1,2 (Akt-I) induced an increase in the rate of nuclear influx of both Foxo1-GFP and Foxo3A-GFP. The difference between the relative increases of Foxo1-GFP and Foxo3A-GFP can be seen in figure **B** in which the scale is 20 fold that of the same experiment in figure A. (**C**) Representative confocal images of a single muscle fiber expressing Foxo3A-GPF treated with 40 nM LMB with or without Akt-I for the times indicated. Nuclear Foxo3A-GFP increases with LMB treatment revealing nuclear import. With Akt inhibition nuclear import increases indicating cytoplasmic retention to be Akt-dependent. (**D**) Unlike the Z-line distribution of Foxo1-GFP (**see Figure 2.1**), Foxo3A-GFP appears as a doublet.

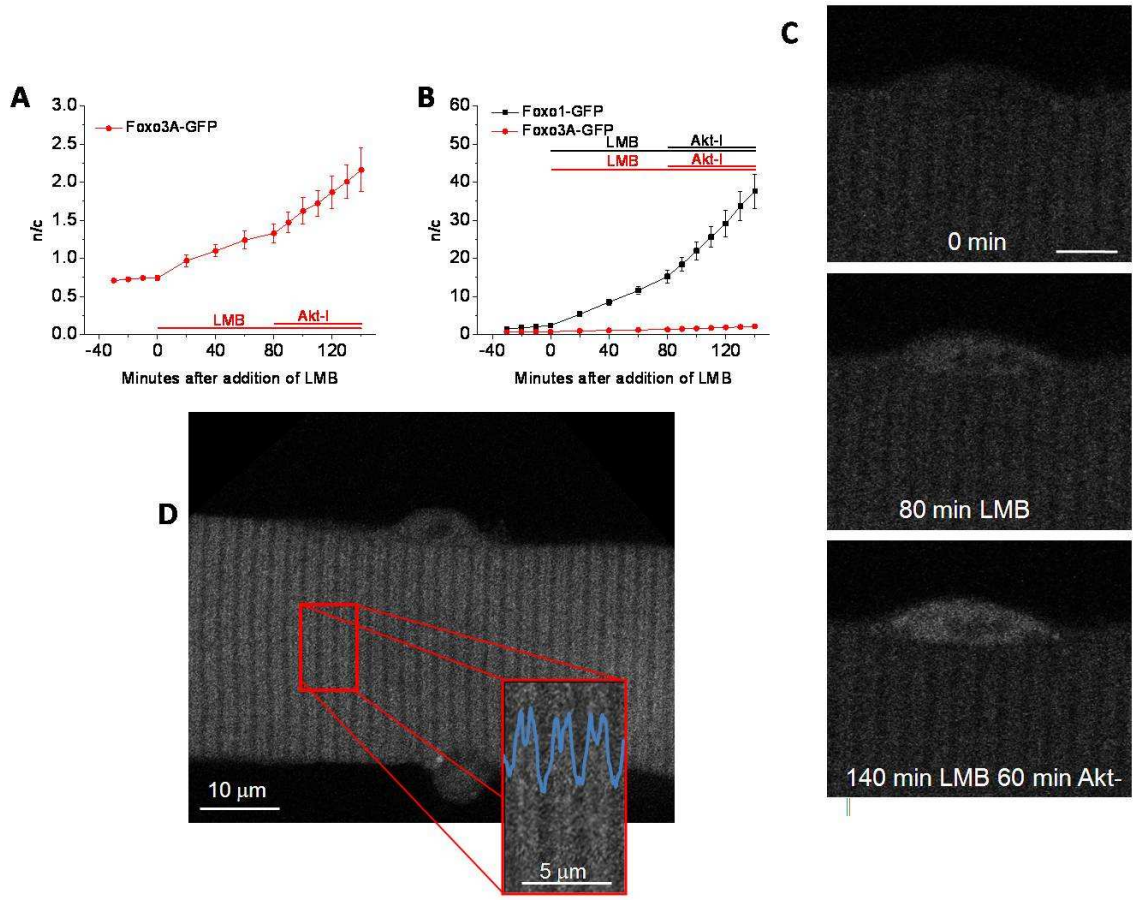

The basis for the much slower nuclear influx exhibited by Foxo3A compared to Foxo1 will be considered in the discussion.

We also noted that the sarcomeric pattern of distribution of Foxo3A was different from that of Foxo1. Whereas Foxo1-GFP was localized in a single sharp line per sarcomere at the sarcomeric Z-lines (**Figure 2.1B**), Foxo3A-GFP is present in a doublet band per sarcomere on either side of the Z-line (**Figure 2.8D**).

9. Rate of unidirectional nuclear influx

To determine the effect of kinase activity on the unidirectional rate constants for movement of cytoplasmic Foxo-1-GFP out of the cytoplasm and into the nucleus, after a control period of 30 minutes we pretreated fibers with LMB for 40 minutes and then added staurosporine or IGF-1 for an additional 120 minutes (**Figures 2.9A-B**). The average rate of increase of nuclear fluorescence in LMB alone was 0.14 n/c per minute and the average ratee in LMB with staurosporine was 0.31 n/c per minute (**Figure 2.9A**), indicating that in the absence of staurosporine, kinase activity reduced the rate of nuclear influx of Foxo1, presumably by maintaining the concentration of dephosphorylated Foxo1 at slightly less than half of the concentration attained in the presence of staurosporine. Note that specific inhibition of Akt by Akt-I-1,2 caused a similar (approximately 2-fold) increase in the rate of Foxo1-GFP nuclear influx in the presence of LMB, confirming that Akt is the predominant kinase phosphorylating cytoplasmic Foxo1 in muscle fibers. As anticipated, IGF-1 treatment completely ablated nuclear influx (**Figure 2.9B**).

Figure 2.9 Nuclear influx rate constant with staurosporine and IGF-1.

Quantification of the slope measured in nuclear/cytoplasmic (n/c) per minute in fibers treated with LMB followed by staurosporine (**A**; n=5) or IGF-1 (**B**; n=5) treatment is the rate of nuclear influx induced by these individual treatments. (**C**) The rate constant of nuclear influx k of the first 40 minutes compared to the last 80 minutes of the 120 minute time course of LMB treatment is the same during LMB treatment alone (n=4). (**D**) k increases significantly during 80 minutes of staurosporine treatment from k during LMB treatment alone (n=10; * $P < 0.05$). (**E**) IGF-1 causes a significant decrease in k in comparison to k during the control period with LMB alone (n=11; * $P < 0.05$). Data represented as means ± SE.

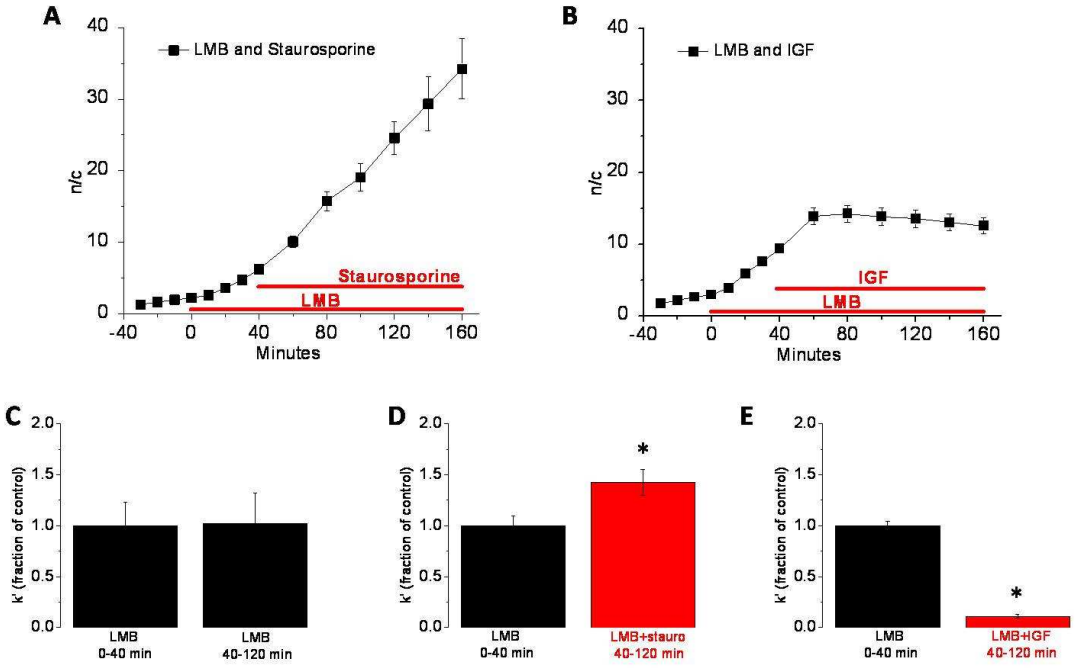

10. First order rate constants for unidirectional cytoplasmic to nuclear fluxes

We next calculate the apparent first order rate constant k' for unidirectional flux of Foxo from the cytoplasm to the nuclei for the experiment in **Figure 2.9**. Using Appendix Eqn (A4), k' can be evaluated from successive images acquired at times t_1 and t_2 using the equation:

$$k' = [2/(c_1+c_2)]\,[(n_2-n_1)/(t_2-t_1)]\,(V_n / V_c), \qquad \text{(Eqn 1)}$$

where n_i is the mean pixel fluorescence of the nucleus at a specified time t_i and c_i is the mean cytoplasmic pixel fluorescence at the same specified time. The value used for V_n / V_c was the mean value of $-\Delta c/\Delta n$ of 0.049 (+/- 0.0079) obtained from 11 fibers during Foxo1-GFP nuclear influx over time periods sufficient to give relatively large values of Δc (see above). To assess the consistency of k' during fiber treatment with LMB, we

calculated k’ for data values collected at t_1 of 0, 20, 40, 60, 80, and 100 minutes after LMB addition using the corresponding respective values collected at t_2 of 20, 40, 60, 80, 100, and 120 minutes after LMB addition. This yielded 6 consistent k' values, demonstrating the uniformity of k’ under these conditions (data not shown). Next, we calculated the average k' for the first 40 minutes and last 80 minutes of each group of experiments by averaging the individual k's calculated per fiber. We then compared these two data sets within each of the three sets of experimental conditions by normalizing all k' values to the mean k' of the control period (0-40 minutes), thus calculating the k' of the experimental condition (40-120 minutes) as a fraction of k' during the control period. The mean k' in the first 40 minutes in LMB treatment alone was then compared to the mean k' for the next 80 minutes of treatment with LMB and a phosphorylation modulator as a fraction of the LMB alone control period (**Figures 2.9C-E**). We saw a modest but significant increase in k’ with staurosporine treatment (**Figure 2.9D**) and a more drastic and significant decrease in k’ with IGF-1 (**Figure 2.9E**) whereas fibers treated with LMB alone for the same time showed no difference in their k’ values in the first 40 minutes in comparison to the last 80 minutes (**Figure 2.9C**).

The ratio of the apparent rate constant for nuclear influx during treatment with LMB plus a phosphorylating or a dephosphorylating agent to the rate constant for nuclear influx with LMB alone should be proportional to the fraction of control dephosphorylated Foxo1 that is present in the cytoplasm in the presence of the additional agent, assuming that only unbound dephosphorylated cytoplasmic Foxo1 is imported into the nucleus, that the percent of cytoplasmic dephosphorylated Foxo1-GFP that is not bound to cytoplasmic sites is the same in the 2 conditions and that the nuclear transport system itself is not

altered by the experimental manipulation. During staurosporine treatment the fraction is 1.4, indicating that general inhibition of phosphorylation by staurosporine caused a 40% increase in the cytosolic concentration of dephosphorylated Foxo1. In sharp contrast, during IGF-1 treatment the fraction is 0.11, indicating a decrease of cytosolic dephosphorylated Foxo1 to 11% of its control level prior to IGF-1 treatment, or a phosphorylation of 89 % of the control dephosphorylated Foxo1 on the application of IGF-1. These values, obtained from the kinetic analysis, provide a quantitative measure of the extent to which the inhibition of kinase activity by staurosporine promotes the dephosphorylation of cytoplasmic Foxo1 and IGF-1 promotes its phosphorylation (**Figures 2.9C-E**).

11. Akt is necessary for IGF-1-induced cytoplasmic retention of Foxo1

To determine the role of Akt in the reduction of nuclear Foxo1 due to IGF-1 treatment, we determined the rate of nuclear influx during inhibition of Akt in the presence or absence of IGF-1. This experiment had four distinct segments (**Figure 2.10A**). First, a control period of 30 minutes with no added agents. Second, 80 minutes treatment ("0 to 80 min") with LMB. Third, 40 minutes ("80 to 120 min") exposure to 1 μM Akt inhibitor Akt-I-1,2 in the continued presence of LMB. Up to this point all fibers were exposed to the same reagents. Then, in the fourth segment, fibers were treated with or without IGF-1 for 80 minutes ("120 to 200 min"). Note that media was not changed during the entirety of this experiment and therefore no reagents were removed. The results showed that the rates of nuclear influx with and without IGF-1 in the presence of Akt inhibitor were the same (**Figure 2.10A**), indicating that the entire IGF-1 effect is mediated by Akt and that Akt activity is necessary for IGF-1-induced reduction of nuclear Foxo1. Furthermore, the

calculation of the apparent rate constants of cytoplasmic efflux of Foxo1-GFP (k'), as described above, for the last three segments at 0-80, 80-120, and 120-200 minute showed IGF-1 treatment to be ineffective in changing the rate constant of cytoplasmic efflux when Akt was inhibited (**Figure 2.10B**). As expected for two samples subjected to the same treatment, the rate constants of nuclear influx from both samples from 0-80 minutes were not significantly different, nor were the rate constants of nuclear influx different for both samples from 80-120 minutes. Of note, the last time segment did not have significantly different k's, regardless of the presence or absence of 100 ng/ml IGF-1, revealing Akt inhibition to be sufficient to fully suppress the IGF-1 effect of reducing nuclear influx of Foxo1.

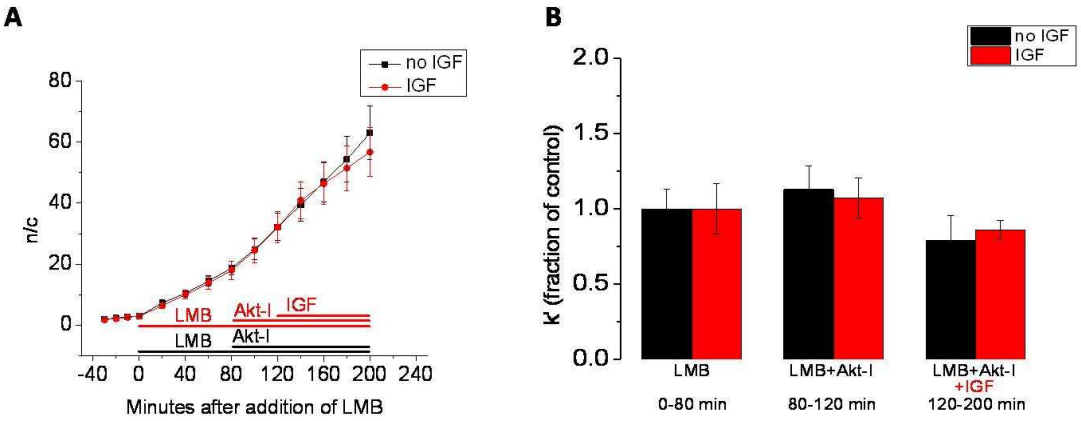

Figure 2.10 Akt modulation of IGF-1.

(**A**) Quantification of the slope measured in nuclear/cytoplasmic fluorescence (n/c) per minute in fibers treated with LMB followed by Akt-I-1,2 (Akt-I; n=12) or Akt-I-1,2 and IGF-1 (n=13) shows inhibition of Akt to prevent the decrease in the rate of nuclear influx normally induced by IGF-1. (**B**) A comparison of the nuclear influx rate constants at 0-80 minutes, 80-120 minutes, and 120-200 minutes of LMB treatment and additional treatment of Akt-I-1,2 and IGF-1 as labeled. The fibers represented in black were treated with LMB with Akt-I-1,2 (n=12) and those in red were treated with LMB, Akt-I-1,2, and IGF-1 (n=13). Data represented as means ± SE.

D. DISCUSSION

Foxo transcription factors play key roles in cell proliferation, cell cycle and cellular survival, and are expressed in all cells of the human body (6, 46, 75). In skeletal muscle, Foxo proteins play a key role in determining muscle size through the regulation of transcription of atrogene products such as E3 ubiqutin ligases atrogin-1/MAFbx and MuRF-1 (19, 53, 56).

Here, we utilize confocal imaging of fluorescence from exogenously expressed Foxo-GFP to monitor kinetics of nuclear-cytoplasmic movements of Foxo proteins in living muscle fibers. Comparison of antibody-stained endogenous Foxo1 and exogenously expressed Foxo1-GFP in terms of sarcomeric localization (**Figure 2.1**), nuclear/cytoplasmic distribution (**Figure 2.2A**), and response to treatment (**Figures 2.4E and F**) validate this system of adenovirally expressed Foxo-GFP as a reliable indicator of endogenous Foxo and as a useful tool in measuring rates of nuclear-cytoplasmic translocation in studies involving fluorescently-tagged Foxo.

Our results with Foxo1-GFP show that IGF-1 treatment alone is sufficient to prevent nuclear targeting of Foxo1 in live adult skeletal muscle fibers, and demonstrate the necessity of the kinases PI3K and Akt in cytoplasmic retention of Foxo1 (**Figures 2.3A, 2.3C, 2.4A, 2.4C, and 2.4D**). Furthermore, we identify Akt's functional activity to be necessary to the decrease in nuclear Foxo1 that occurs in response to IGF-1 treatment (**Figure 2.10**). Kinases such as SGK, CK1, and DYRK1A have been shown to be Foxo kinases (10-12) but do not seem to be sufficient for modulating the Foxo1 nuclear-cytoplasmic movements monitored in cultured adult muscle fibers.

PP2A directly dephosphorylates Foxo1 in NIH T3T cells (14). The impressive decrease in nuclear Foxo1 in response to inhibition of PP2A via OA (**Figure 2.5**) demonstrates PP2A's functional role in Foxo1 dephosphorylation in skeletal muscle, as well. Studies of unidirectional nuclear influx with and without OA treatment identify PP2A inhibition to occur in the cytoplasm (**Figure 2.6E**). This does not limit PP2A's role to the cytoplasm but does reveal the importance of its cytoplasmic activity, as well as its role in nuclear-cytoplasmic cycling of Foxo1.

A kinetic reaction scheme representing the nuclear-cytoplasmic movements of Foxo proteins is presented in **Figure 2.11**, together with the signaling systems and inhibitors that we have examined as modifiers of Foxo movements in our muscle fiber studies. Other physiological modulators of Foxo movements, such as Foxo phosphorylation at other sites (10, 11) or acetylation (32) are not shown in **Figure 2.11** and can be thought of as providing a possible constant background level of modulation of the Foxo fluxes observed here. Dephosphorylated cytoplasmic Foxo is unidirectionally translocated out of the cytoplasm by the nuclear localization signal (NLS) and Ran GTPase driven nuclear import system, but phosphorylated Foxo is not transported by this system (18). Note that the rate constant k for unidirectional first order flux of dephosphorylated Foxo out of the cytoplasm and into the nucleus in **Figure 2.11** is the same as the k in Eqn (A1). In contrast to the nuclear import system, which carries only dephosphorylated Foxo, phosphorylated but not dephosphorylated Foxo is carried by the CRM1 dependent nuclear export system, with export facilitated by the chaperone protein 14-3-3 (7).

The nuclear export of Foxo can be inhibited by LMB (**Figure 2.11**), which binds to and thus removes the availability of CRM1 for nuclear export. In the presence of a fully

blocking concentration of LMB any Foxo that enters the nucleus is unable to leave and becomes trapped in the nucleus. Inhibition of nuclear export via LMB thus provides a powerful tool for measuring the rate of unidirectional nuclear influx and for calculating its rate constant of cytoplasmic efflux. The change in the rate constant for unidirectional efflux out of the cytoplasm due to treatment with phosphorylation modulators demonstrates the importance of cytoplasmic phosphorylation/dephosphorylation of Foxo1 in regulation of its rate of cytoplasmic efflux (**Figures 2.6, 2.9, and 2.10**). Furthermore, the increase in the rate of nuclear influx that resulted from staurosporine addition in the presence of LMB (**Figure 2.9A**) indicates that the nuclear import machinery is not saturated at the level of expression of Foxo1-GFP employed under our conditions of infection by adFoxo1-GFP. Based on the important information obtained here and elsewhere with the nuclear export inhibitor LMB, identification of a comparable specific inhibitor of nuclear import would further open up the field to understanding the kinases and phosphatases that regulate Foxo1 nuclear export.

It should be noted that the same unidirectional flux of Foxo from muscle fiber nuclei can be considered as either a unidirectional efflux out of the cytoplasm or as a unidirectional influx into the nuclei. In practical terms of ease of experimental measurement, it is more convenient to monitor the rate of change of Foxo-GFP fluorescence in the nuclei than in the cytoplasm. The total volume of the nuclei is much smaller than that of the cytoplasm, so the corresponding change in mean pixel fluorescence for a given flux of Foxo-GFP between cytoplasm and nuclei is much larger in the nuclei than in the cytoplasm. By conservation of mass, the ratio of changes of nuclear to cytoplasmic mean pixel fluorescence for a given movement of Foxo-GFP between nuclei and cytoplasm is equal

to the ratio of cytoplasmic to nuclear volume in the muscle fibers. However, in terms of mechanistic interpretation of the nuclear import system, it is more appropriate to consider cytoplasmic rather than nuclear concentration change and the rate of efflux of Foxo out of the cytoplasm. This is because the unidirectional flux of Foxo from cytoplasm to nuclei is determined by the cytoplasmic concentration of dephosphorylated unbound Foxo, and is independent of the nuclear concentration, as indicated in the kinetic scheme in **Figure 2.11** and by Eqn (A1).

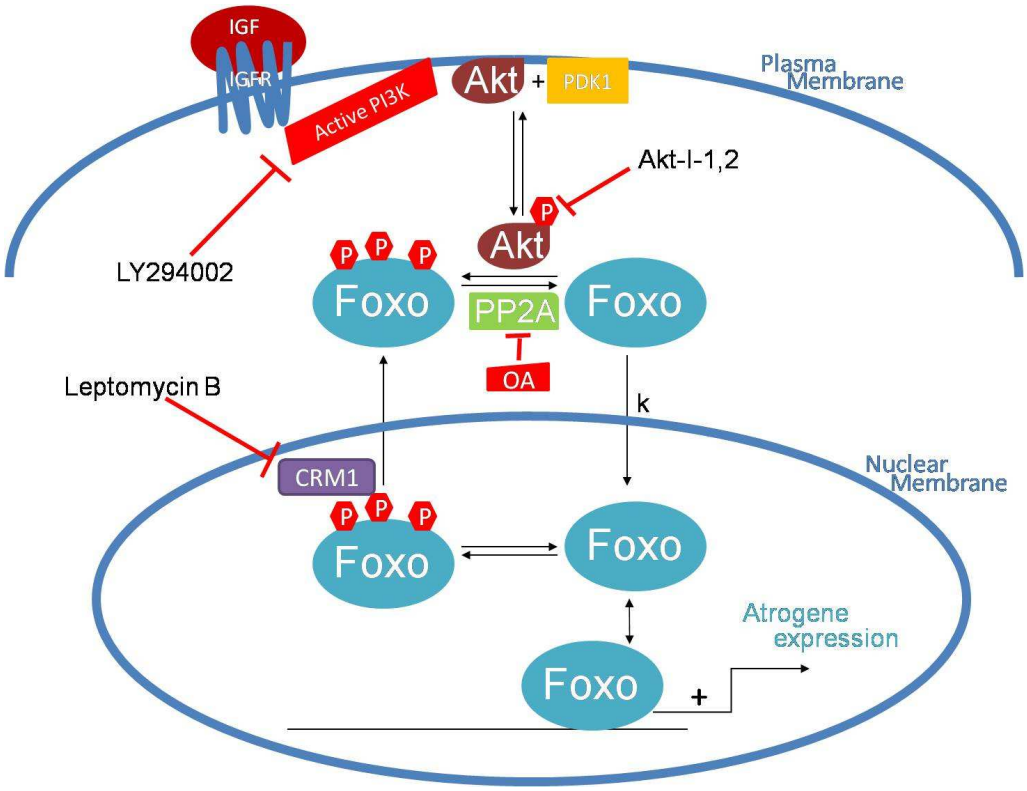

Figure 2.11 Schematic presentation of regulators of subcellular localization of Foxo.

Nuclear-cytoplasmic trafficking is regulated by phosphorylation of Foxo by active Akt. Binding of IGF to its membrane bound receptor IGFR activates the kinase PI3K, indirectly causing the phosphorylation of Akt, which directly phosphorylates Foxo. Inhibition of PI3K by LY294002 or inhibition of Akt by Akt-I-1,2 prevents phosphorylation of Foxo and thus induces nuclear import of Foxo. CRM1 facilitates of nuclear export of Foxo1 and inhibition of CRM1 by Leptomycin B prevents nuclear export of Foxo.

The unidirectional rate constant of cytoplasmic efflux of Foxo1 is relatively high compared to that of other transcription factors that our laboratory has studied. Based on the nuclear influx measured in the presence of LMB, the apparent first order rate constant k' for unidirectional flux of Foxo1-GFP out of the cytoplasm and into the nucleus was 0.355 +/- 0.035 per hour under resting conditions (data from **Figure 2.10**). In contrast, under resting conditions, the transcription factor NFATc1 leaves the cytoplasm and enters the nucleus at a much slower rate. As determined in LMB, the unidirectional flux of NFATc1 from cytoplasm to nucleus occurs with an apparent first order rate constant of 0.074 +/- 0.005 per hour (based on data used to make Figures 2C and 6C in Shen et al., 2006, reference 76), assuming V_n/V_c is the same for Foxo1 and NFATc1. Foxo3A also enters the nucleus much more slowly than Foxo1. The unidirectional first order apparent rate constant for movement of Foxo3A out of the cytoplasm and into the nucleus is 0.023 +/- 0.004 per hour in the presence of LMB (calculated from the data for nuclei in fibers in **Figure 2.8**). One possible explanation for the lower unidirectional apparent rate constants for movement of NFATc1 and Foxo3A out of the cytoplasm compared to the rate constant for Foxo1 could be their less effective transport by the nuclear import system, ie, the actual rate constant k, would be considerably lower for Foxo3A or NFATc1 than that for Foxo1, but this may be unlikely for the similar molecules Foxo1 and Foxo3A. Alternatively, the fractional dephosphorylation of NFATc1 or Foxo3A in the cytoplasm might be much lower than that of Foxo1. A much lower relative degree of dephosphorylation of Foxo3A than Foxo1 in muscle fibers would be consistent with the observation that nerve growth factor (NGF) activated Foxo phosphorylation in PC12 cells occurs at considerably lower NGF

levels for Foxo3 than for Foxo1(44). Finally, the fraction of unbound dephosphorylated Foxo1 in the cytoplasm could be considerably greater than the fraction of unbound dephosphorylated Foxo3A or NFATc1 in the cytoplasm. Intriguingly, the sub-sarcomeric distribution pattern for Foxo3A is different from that of Foxo1, possibly indicative of a difference in binding and fraction bound. The presence of two Foxo isoforms, Foxo1 and 3A, having about 20-fold different nuclear-cytoplasmic shuttling rates under control conditions, but presumably modulating the expression of the same group of genes, raises interesting questions regarding mechanism, regulation, and function that merit future investigation of Foxo isoforms.

E. Appendix:

Apparent first order rate constant for unidirectional flux of Foxo from cytoplasm to nuclei

Assuming that the rate of nuclear efflux is 0 with LMB treatment, that the movement of Foxo-GFP out of the cytoplasm is a first order process, and that only depohsphorylated and unbound Foxo-GFP can enter the nucleus, the rate of change of cytoplasmic Foxo-GFP fluorescence due to movement of Foxo-GFP out of the cytoplasm is given by:

$$dc/dt = -k f_c c, \qquad \text{(A1)}$$

where c is the mean pixel fluorescence in the cytoplasm, t is time, k is the first order rate constant for movement of dephosphorylated and unbound Foxo-GFP from the cytoplasm to the nucleus and f_c is the fraction of total cytoplasmic Foxo-GFP that is both

dephosphorylated and unbound. Defining the apparent rate constant k' as k f_c, k' is given by

$$k' = -(1/c)\,(dc/dt)\,. \qquad \text{(A2)}$$

Rearranging the equation for conservation of mass (Eqn 1; in Results, above) and taking the time derivative gives

$$dc/dt = -(dn/dt)\,(V_n / V_c) \qquad \text{(A3)}$$

Substitution of Eqn (A3) into Eqn (A2) gives the equation

$$k' = (1/c)\,(dn/dt)\,(V_n / V_c) \qquad \text{(A4)}$$

for the apparent first order rate constant for Foxo-GFP movement out of the cytoplasm and into the nuclei.

CHAPTER 3

OVEREXPRESSION OF FOXO1 PREVENTS MUSCLE CONTRACTION IN SKELETAL MUSCLE

A. Introduction

The process by which electrical stimulation of a muscle fiber initiates muscle contraction is termed excitation-contraction (EC) coupling. This process begins with depolarization of the fiber causing an action potential which is propagated both axially and inwardly primarily via current through Nav1.4, the skeletal muscle isoform of the voltage-gated sodium channel, all along the sarcolemma and through the transverse (T-) tubule system of the fiber (64, 65). The depolarization of the cell membrane induces conformational changes in the Dihydropyridine receptors (DHPRs) which are mechanically coupled with skeletal muscle Ryanodine receptor Ca^{2+} release channels (RyR1) in the sarcoplasmic reticulum (SR). The RyR1 channels mediate rapid Ca^{2+} release from the sarcoplasmic

reticulum (SR) into the cytosol leading to Ca^{2+} binding to thin filament troponin C and activation for contraction (61-63).

The family of Forkhead box O (Foxo) transcription factors, of which Foxo1 is a member, is evolutionarily conserved and characterized by a 100-residue DNA-binding region called the Forkhead domain. In skeletal muscle, Foxo transcription factors control muscle atrophy/hypertrophy by promoting transcription of ubiquitin ligases. Upregulation of either of two isoforms of Foxo, Foxo1 and Foxo3A (also referred to as Foxo3), is independently sufficient to induce muscle atrophy (19, 38). Knockout of Foxo1 is embryonic lethal and tissue-specific induced knockout of Foxo1 results in tumor growth (39, 48). Foxo3 has been shown to regulate both lysosomal and proteasomal degradation through transcriptional regulation of atrogenes, proteins that induce muscle atrophy, such as atrogin-1/MAFbx, MuRF-1, LC3, and Bnip3 (25, 60).

Here, we identify a novel role of Foxo1 in control of excitation of muscle. Using exogenously expressed Foxo1-GFP in cultured adult flexor digitorum brevis (FDB) muscle fibers we have determined that overactivity of Foxo1 prevents SR calcium release and the subsequent muscle contraction. However, the morphology of the T-tubule system is not altered and the overall health of the fiber does not appear compromised. We further identify reduction in the expression of the sodium channel Nav1.4 to be a likely cause of the inability of fibers to respond to electrical stimulation.

B. Methods

1. Muscle fiber culture and infection

Culture of flexor digitorum brevis (FDB) and infection were carried out as detailed in (77). Briefly, the muscle was isolated from CD-1 mice, enzymatically dissociated with collagenase type I (Sigma-Aldrich) in MEM (Invitrogen, Carlsbad, CA) with 10% FBS, and 50 µg/ml gentamicin for 2 hours at 37˚. Muscle was then gently triturated to separate fibers in MEM with FBS and gentamicin. Fibers were plated in in MEM laminin-coated glass-bottom dishes containing lysate with adenovirus coding for GFP or Foxo1-GFP (a gift from Dr. Joseph Hill, University of Texas Southwestern Medical Center 67). Fibers treated with IGF-1 (Sigma Aldrich, St. Louis, MO) were plated in a dish containing 100 ng/ml IGF-1 in addition to lysate and this concentration of IGF-1 was maintained for the entirety of the experiments.

2. Indo-1 ratiometric recordings

Indo-1 acetoxymethyl (AM) ratiometric recording and analysis were performed as previously described (Hernandez-Ochoa EH et al., 2012) but with some modifications for loading. Briefly, cultured FDB fibers were loaded with Indo-1AM (2 µmol/L for 60 min at 22°C; Invitrogen) in L-15 media (ionic composition in mM: 137 NaCl, 5.7 KCl, 1.26 CaCl2, 1.8 MgCl2, pH 7.4; Invitrogen) . Then the fibers were washed thoroughly with appropriate L-15 media to remove residual Indo-1AM. The culture dish was mounted on an Olympus IX71 inverted microscope and viewed with an Olympus 60×/1.20 NA water immersion objective. Fibers were illuminated at 360 nm, and the fluorescence emitted at 405/30 and 485/25 nm was detected simultaneously. The emission signals were digitized

and sampled at 10 Hz using a built-in AD/DA converter of an EPC10 amplifier and the acquisition software Patchmaster (HEKA Instruments Inc., Bellmore, NY, USA). Field stimulation (1 ms, 8 V, alternating polarity) was provided by a custom pulse generator through a pair of platinum electrodes. The electrodes were closely spaced (0.5 mm) and positioned directly above the center of the objective lens, to achieve semi-local stimulation.

3. Transverse tubular network imaging in living fibers

Control, GFP or Foxo1-GFP fibers were stained with the voltage-sensitive dye pyridinium, 4-[2-(6-(dioctylamino)-2-naphthalenyl) ethenyl]-1-(3-sulfopropyl)-, inner salt (di-8-ANEPPS) (2.5 μmol/L; in L-15 media for 1 h) and imaged on a Fluoview 500 confocal system (Olympus; ×60, 1.3 NA water-immersion objective; pixel dimensions 0.2 × 0.2 μm in x and y). Confocal images of the tubular network were obtained with 512 × 512 pixel x–y images (average of eight images). Images were collected from randomly selected fibers using the same image acquisition settings and enhancing parameters. Images were background corrected and a region of interest of fixed dimensions was used to estimate average fluorescence profile within the region of interest.

4. Action Potential recordings

Potentiometric dye action potential recordings and analysis were performed as previously described but with some modifications (78). FDB fibers were stained with 2.5 μM di-8-ANEPPS in the incubator for 3 hrs, followed by three washes in L-15 media. Fiber cultures were mounted on a Zeiss LSM 5 LIVE high-speed confocal system and

stimulated with dual platinum field electrodes. Fiber fluorescence was excited with a 532-nm diode laser, and fluorescence emission above 550 nm was sampled during repeated line scans through the interior of fibers (100 μs/line). The line scan was conducted at a depth of ~15–20 μm into the interior of the fiber. Significant measures were taken to ensure that resulting signals were propagated APs and not artifacts imposed by stimulation (see results). Signals were converted to $-\Delta F/F_0$ values, and four trials were averaged to increase the signal-to-noise ratio. APs were triggered using the same 1-ms electrical stimulus as in Ca^{2+} release assays. All single fiber recordings were performed at room temperature, 22°C.

5. Data analysis and statistics methods

Electrophysiology and Indo-1 data were analyzed and plotted using Patchmaster, Fitmaster (HEKA Instruments Inc.). Immunocytochemistry, di-8-ANEPPS signals and Western blot data were analyzed with ImageJ. Further data evaluation and statistical analysis were conducted using OriginPro 8 software (OriginLab Corporation, Northampton, MA, USA). Summary data were reported as mean ± SEM when samples followed normal distributions and as medians when sample distributions were less well defined. Box plots and bar graphs were used for graphic illustration of data. Statistical significance was assessed using either parametric two sample t-test or with the non-parametric Mann–Whitney rank-sum test for unpaired data sets.

6. Western blotting

Protein extraction and western blotting techniques were performed as described in Schachter et al. (77) with slight modifications. Briefly, FDB fibers were infected and

cultured for 2 days and treated with IGF-1 when indicated. One or two fibers were then collected from each dish and mixed with 14 µl M-PER (Thermo Scientific, Rockford, IL), a protease inhibitor cocktail (Roche Diagnostics, Indianapolis, IN), 3.7 µl sample reducing agent, and 9.25 µl LDS sample buffer (Invitrogen). This mixture was pipetted up and down to lyse fibers, heated at 70° for 10 min, and run on a NuPAGE Novex 3- 8% Tris gel (Invitrogen). Proteins were transferred to a PVDF membrane. Skm1 (referred to as Nav1.4; Sigma) and α-actinin antibodies (Sigma) were used and then the membrane was treated with ECL and film was exposed and developed.

C. Results

1. Fibers expressing Foxo1-GFP appeared healthy and responsive to chemical stimulation

Fibers expressing Foxo1-GFP appeared normal with the clearly visible striations that give rise to the skeletal and cardiac muscle alternative name - striated muscle (**Figure 3.1**). These fibers also demonstrated functional Foxo1-GFP signaling in response to treatment with IGF and kinase inhibitors, as previously described in Schachter et al., 2012. Furthermore, nuclear/cytoplasmic distribution of endogenous Foxo1 and exogenously expressed Foxo1-GFP was essentially the same. This indicates that Foxo1 regulation is intact in fibers expressing Foxo1-GFP. Importantly, exogenous Foxo1 expression was merely 7-fold that of endogenous Foxo1 expression (77). Overall, these fibers look healthy and typical for cultured fibers.

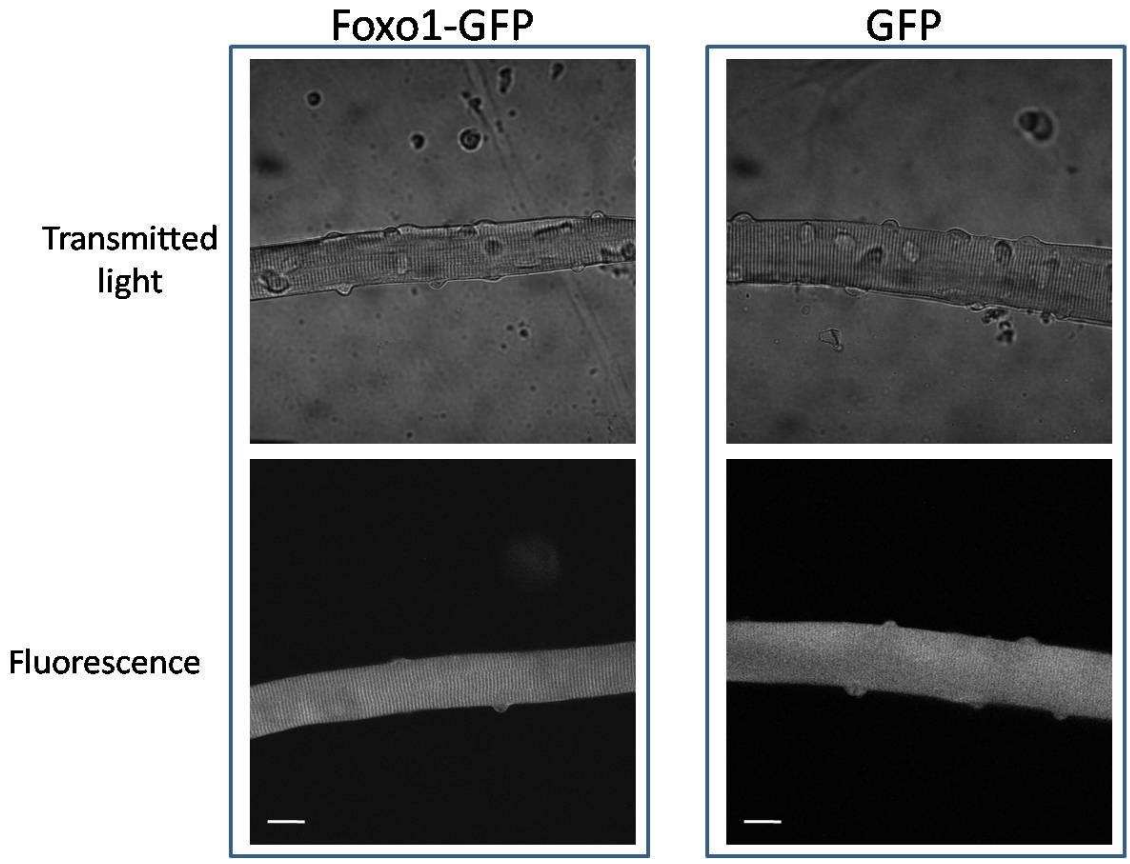

Figure 3.1 Fibers expressing Foxo1-GFP appear normal.

Signs of health are visible: striations, nuclei are predominantly peripheral, and fibers are smooth and straight. Scale bars are 20 µm.

2. Foxo1 suppresses stimulation induced calcium transient

Although Foxo1-GFP fibers appeared healthy and biochemically functional, they responded to electrical stimulation in an abnormal manner. Control fibers with or without GFP expression stimulated for 1 msec at 25 V and a train of pulses at 100 Hz showed robust calcium transients (**Figure 3.2 A, C**) and contraction (data not shown). In stark contrast, Foxo1-GFP fibers from the same muscle generally did not respond (**Figure 3.2 B**) and contraction (data not shown). The average change in Indo1 ratio in

response to a single electrical stimulusof 25 V in fibers expressing Foxo1-GFP (referred to here as Foxo1-GFP fibers) was approximately 10% that of control fibers or fibers expressing GFP (referred to here as GFP fibers; **Figure 3.2D**). Another factor that is correlated with the overall health of a fiber is the resting calcium concentration. Control, Foxo1-GFP, and GFP fibers all had basal Indo-1 ratios that were not significantly different, indicating that calcium resting concentrations are not altered by Foxo1 (**Figure 3.2E**).

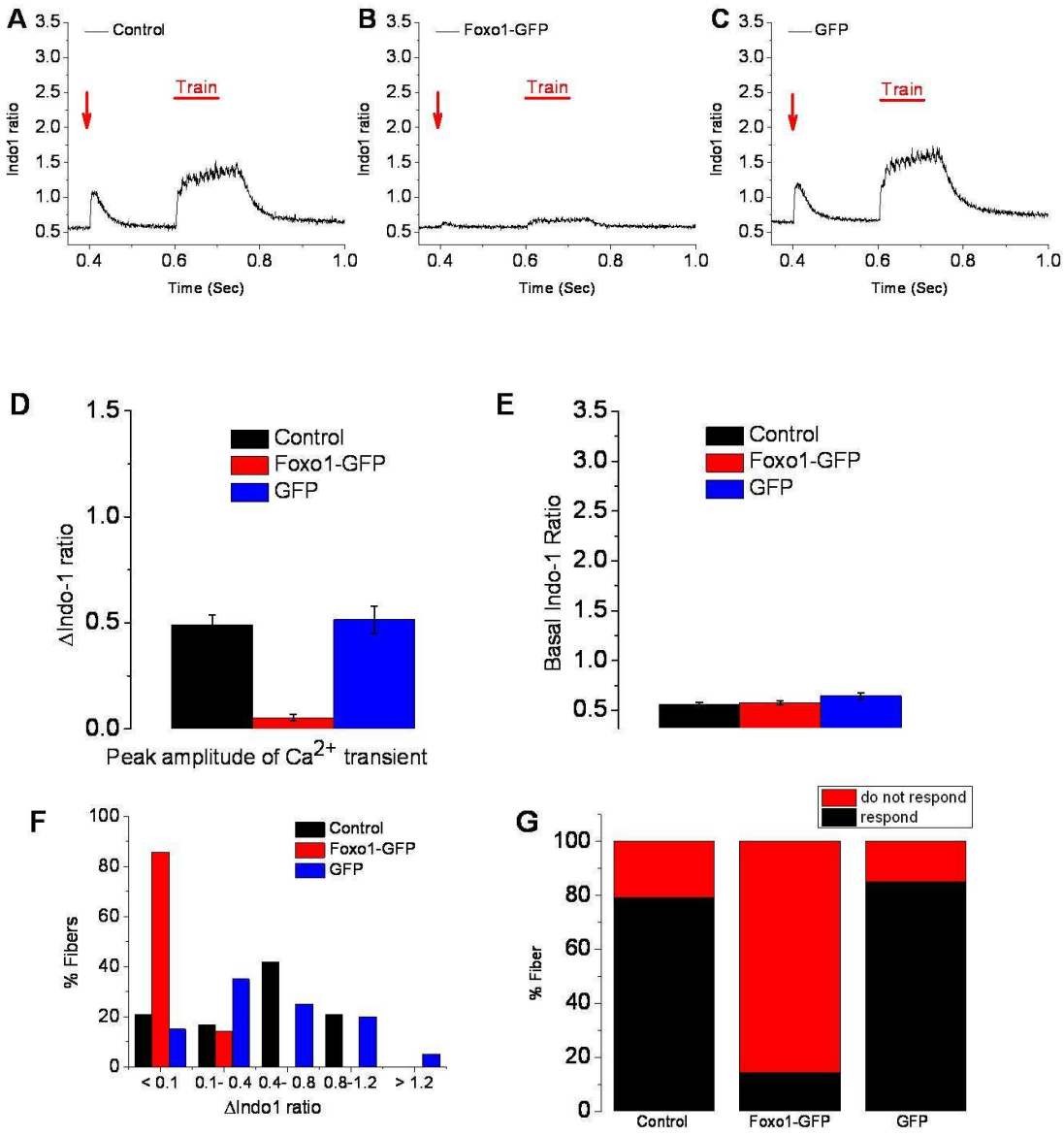

Figure 3.2 Calcium transients are ablated in fibers overexpressing Foxo1-GFP

A Control fibers (n=24) exhibit calcium transients in response to a single 25 V pulses with a 1 msec duration and an electrical train of 100 Hz. **B** Fibers expressing Foxo1-GFP (n=35) do not show calcium transients in response to the same pattern of electrical stimulation. **C** Fibers expressing GFP (n=40) alone respond to electrical stimulation with a calcium transient in a manner consistent with typical healthy FDB fibers. **D** The average change in the Indo-1 ratios of fibers in response to electrical simulation is dramatically decreased in fibers expressing Foxo1-GFP in comparison to control and GFP fibers. **E** Resting rates of calcium are not statistically different in control fibers, fibers expressing Foxo1-GFP, and fibers expressing GFP alone. **F** The distribution of ΔIndo-1 in response to a single stimulus in cultured fibers is a measure of the intensity of

the calcium transient. The majority of Foxo1-GFP fibers have a range of no response to decreased intensity whereas control and GFP fibers have varying degrees of strength. **G** The percent of Foxo1-GFP fibers that exhibited a calcium transient, as defined by peak ΔIndo-1 ratio <0.1, in response to electrical stimulation is significantly lower than that of control fibers and GFP fibers.

While 86% of Foxo1-GFP fibers did not respond to electrical stimulation with a calcium transient at all, a small fraction (14% of Foxo1-GFP fibers) did show a weak increase in cytoplasmic calcium (**Figure 3.2F**). In contrast, only 21% of control fibers and 15% of GFP fibers did not display a calcium transient upon electrical stimulation, and the other fibers displayed responses in a range of strengths (**Figure 3.2F-G**).

3. Foxo1-GFP fibers treated with IGF-1 responded to electrical stimulation

Treatment with IGF-1 prevents nuclear targeting of Foxo1 (15, 77). To determine the role of Foxo1 in response to electrical stimulation, we treated Foxo1-GFP fibers with 100 ng/ml IGF-1 to prevent functional activity of Foxo1 as a transcription factor by keeping it out of fiber nuclei. Remarkably, fibers expressing Foxo1-GFP treated with IGF-1 (referred to here as IGF fibers) responded to electrical stimulation with appropriate calcium transients despite expression of Foxo1-GFP (**Figure 3.3 A-C**). The increase in Indo-1 fluorescence ratio signal in response to electrical stimulation in GFP fibers and IGF fibers were the same, whereas Foxo1-GFP fibers did not exhibit a change in Indo-1 ratio in response to electrical stimulation (**Figure 3.3D-E**). Similar fractions of GFP fibers and of IGF fibers responded to electrical stimulation with strong, weak, or negligible ΔIndo-1 ratio signals, whereas Foxo1-GFP fibers did not exhibit calcium responses and did not contract (**Figure 3.3E**). This indicates that IGF fibers consistently behave in the same manner as control fibers and IGF prevents the impairment developed

in Foxo1-GFP fibers. These results provide evidence that the observed inability of Foxo1-GFP fibers to contract and release calcium results from the functional transcriptional activity that Foxo1 causes.

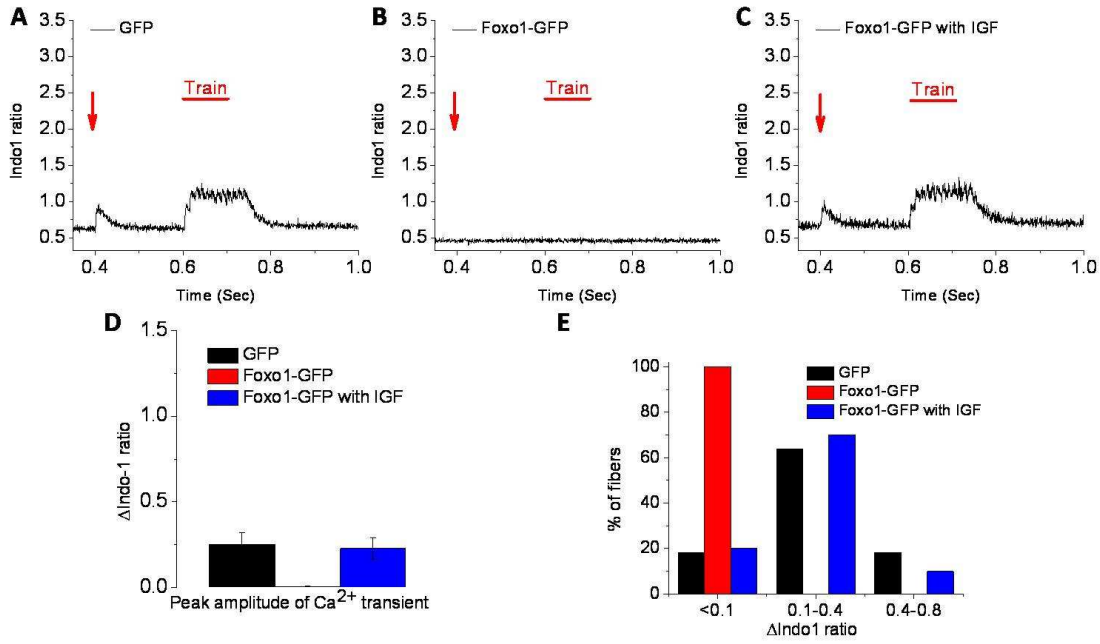

Figure 3.3 IGF-1 treatment prevents Foxo1-induced EC uncoupling.

Cultured fibers expressing GFP (**A**; n=11), fibers expressing Foxo1-GFP **(B;** n=9), and fibers expressing Foxo1-GFP treated with IGF-1 from the time of infection (for 48 hours; **C**; n=10) were stimulated using the same pattern of stimulation as detailed in **Figure 3.2**. Foxo1-GFP fibers treated with IGF-1 did not have compromsed calcium transients as those seen in untreated fibers expressing Foxo1-GFP. **D** The average change in Indo-1 ratio in response to electrical stimulation is significantly reduced in fibers expressing Foxo1-GFP in comparison to fibers expressing GFP alone or fibers expressing Foxo1-GFP and treated with IGF-1. **E** The number of fibers that responded weakly, moderately, and strongly to electrical stimulation that were expressing GFP and those expressing Foxo1-GFP and treated with IGF-1 were comparable in comparison to Foxo1-GFP expressing fibers.

4. T-tubule system remained unaltered

The T-tubule system is a membrane system along which depolarization spreads inward into the fiber. Breakdown of this system disrupts propagation of the action potential and thus the contraction of the fiber. To examine the integrity of the T-tubule system we stained control fibers and Foxo1-GFP fibers with voltage-dependent membrane dye di-8-ANNEPS, which stains the T-tubule system. Imaging these fibers using fluorescence confocal microscopy established that the morphology of the T-tubule system of Foxo1-GFP fibers (**Figure 3.4A**) was unaltered from control fibers (**Figure 3.4B**).

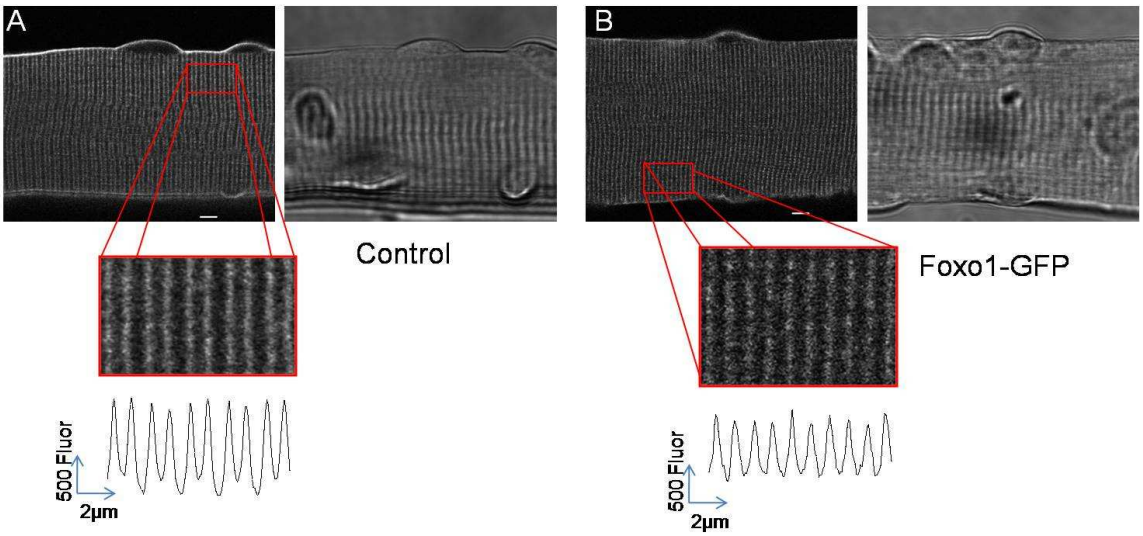

Figure 3.4 T-tubules remain morphologically unaltered

A In control fibers, T-tubules show normal morphology. **B** No changes to normal T-tubule morphology are seen in fibers expressing Foxo1-GFP. Scale bars are 5µm.

5. Fibers expressing Foxo1-GFP failed to propagate action potentials

To further explore the cause of the failure of Foxo1 fibers to contract, we used di-8-ANEPPS to visualize the response to electric stimulation. Both control fibers and Foxo1 fibers appeared the same when stained with this dye (**Figures 3.5A and D**). We determined the response of fibers to external electrical stimulation by taking a continuous line scan image of the fiber before, during, and after stimulation with + - pulses of 14V, 1 ms duration, and then quantifying the fluorescence (**Figure 3.5B-C, E-F**). The fluorescence of di-8-ANEPPS decreased with depolarization of the fiber. Control fibers responded to either positive or negative applied voltage with a decrease in di-8-ANEPPS fluorescence indicating depolarization, reflecting the fact that applied voltage of either polarity generated a depolarizing action potential (**Figures 3.5A-C and G**). In contrast, in Foxo1 fibers, a 1 ms 14V negative applied pulse caused an increase in di-8-ANEPPS signal, while in response to a positive stimulus of 14V, there was a decrease in fluorescence (**Figure 3.5H**). The reversal of signal polarity with the alternation of the pulse polarity is a characteristic of predominantly passive electrotonic polarization due to the field stimulation. Measurement of action potential propagation in control fibers treated with TTX (to inactivate sodium channels) showed a smaller and shorter increase and decrease (appropriate to the polarity) in fluoresce than seen in control fibers untreated with TTX to be an artifact of this system, which lends support to the latter possibility (78). In either case, these results demonstrate that Foxo1-GFP fibers were unable to respond to a change in external voltage by propagating action potentials.

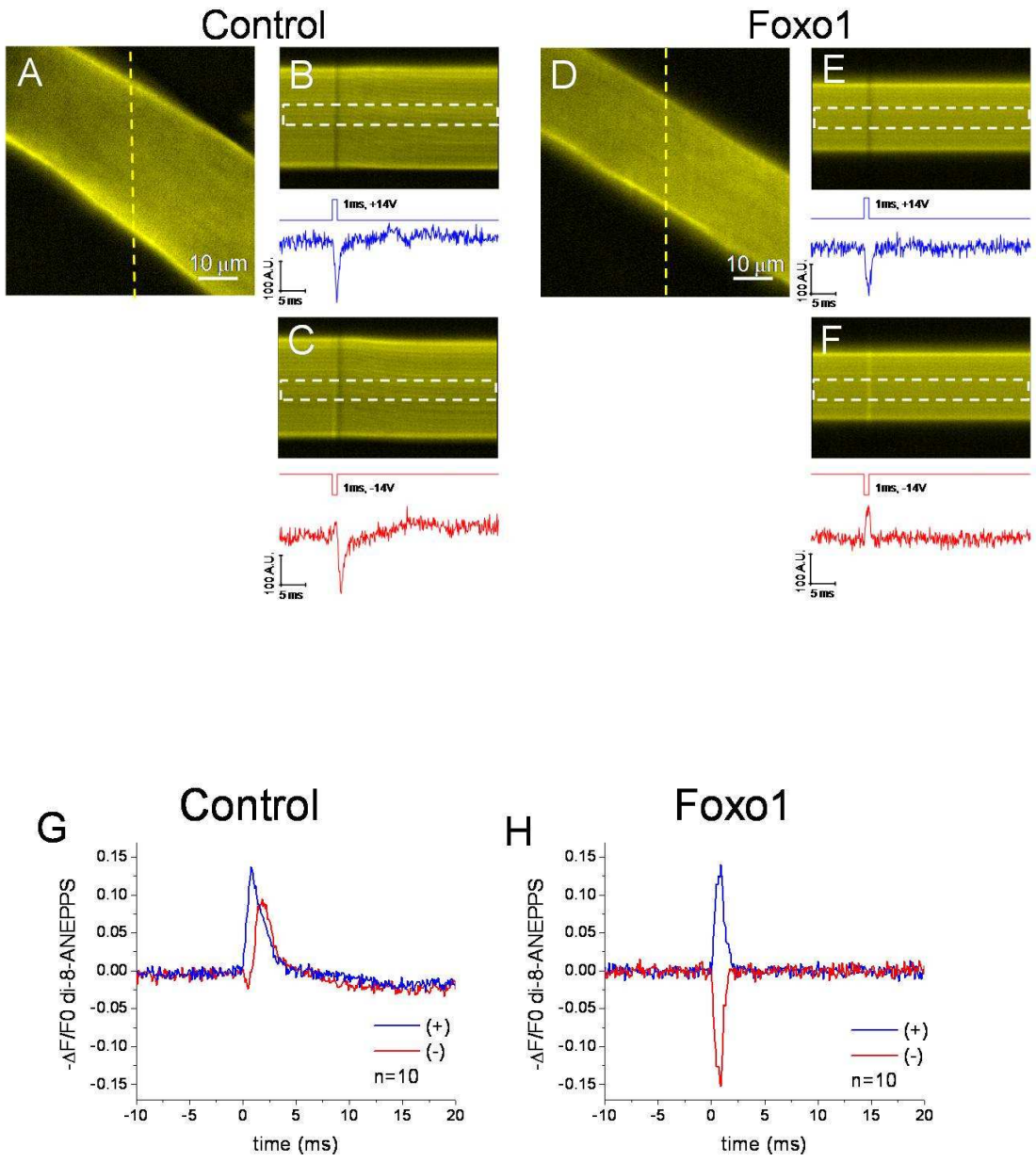

Figure 3.5 Propagation of an action potential is prevented

A, D Representative images of a control fiber **(A)** and a fiber expressing Foxo1-GFP **(D)** stained with the voltage-dependent dye di-8-ANEPPS. Yellow lines in **A** and **D** indicate the areas of the line scan in figures **B** and **C,** and **E** and **F**, respectively. Below figures **B** and **C** are graphs of the change in fluorescence of di-8-ANEPPS in the regions in the white dashed boxes. **G-H** Average change in di-8-ANEPPS fluorescence in control fibers **(G)** and fibers expressing Foxo1-GFP **(H)**.

6. Expression of the sodium channel Nav1.4 was decreased by Foxo1-GFP

Due to the integral role of sodium channels in propagation of an action potential, we explored the possibility that overexpression of exogenous Foxo1-GFP negatively regulated expression of the skeletal muscle sodium channel Nav1.4. To this end, we used western blot analysis of single fibers expressing GFP, expressing Foxo1-GFP, or expressing Foxo1-GFP with IGF-1 treatment. Foxo1 fibers only expressed 32% of Nav1.4 in comparison to GFP fibers. Fibers expressing Foxo1-GFP and treated with IGF-1 had expression levels 57% that of GFP fibers (**Figure 3.6**). We conclude that overexpression of Foxo1-GFP decreases the expression of the sodium channel Nav1.4 and thus prevents depolarization of the membrane and subsequent contraction and calcium release of the muscle fiber. Furthermore, inhibition of nuclear influx of Foxo1 via IGF-1 diminished this effect of Foxo1 on Nav1.4 expression, indicating that the activity of Foxo1 as a transcription factor regulates Nav1.4.

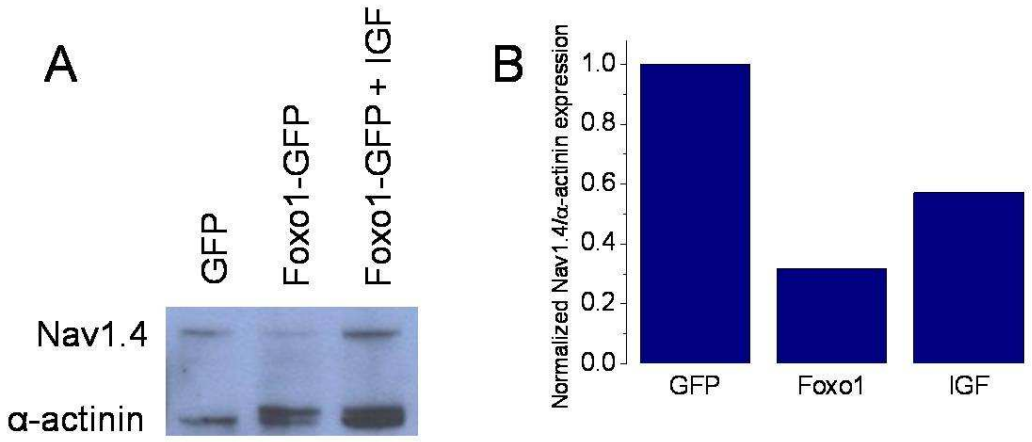

Figure 3.6 Foxo1 activity decreases the expression of the sodium channel Nav1.4

A Western blot of expression of Nav1.4 in fibers expressing GFP, fibers expressing Foxo1-GFP, and fibers treated with IGF-1 expressing Foxo1-GFP. **B** Quantification of western blots show that fibers expressing Foxo1-GFP have decreased expression of

Nav1.4 in comparison to fibers expressing GFP (n=4). IGF-1 treatment of fibers expressing Foxo1-GFP decreased the loss of expression of Nav1.4.

D. Discussion

The transcription factor Foxo1 controls muscle atrophy and regulates the expression of atrogenes such as atrogin and MuRF1 (19, 53, 56). Here, we provide evidence of another role of Foxo1 in the degradation of skeletal muscle. The inability of fibers with overexpression of Foxo1 to contract, activate calcium signaling, or propagate an action potential taken together demonstrate the capacity of Foxo1 to disable functional activity of skeletal muscle (**Figures 3.2, 3.3, and 3.5**).

Cultured muscle fibers overexpressing Foxo1-GFP were structurally normal and demonstrated normal cellular signaling (**Figures 1 and 4** and reference 77). However, these fibers did not respond properly to electrical stimulation: they did not have calcium transients or propagate action potentials (**Figures 3.2, 3.3, and 3.5**). The basal levels of cytoplasmic calcium of fibers expressing Foxo1-GFP were not changed from those of control fibers (**Figure 3.2E**), indicating that the homeostatic mechanisms of calcium regulation were conserved, SERCA was functional, and that the RyR1 was not leaking in fibers expressing Foxo1-GFP. Foxo1 overexpression also did not alter the morphology of the T-tubule system, eliminating the possibility that a cause for the failure of fibers expressing Foxo1 to contract was the inability of current to flow through the T-tubule system **(Figure 3.4)**.

Nav1.4 is an essential part of excitation of skeletal muscle fibers. As such, its regulation is of importance to muscle excitability. The ability of Foxo1 to inhibit expression of

Nav1.4 (**Figure 3.6**) shows the involvement of Foxo1 in another aspect of regulation of skeletal muscle health (**Figure 3.7**). This is supported by a recent finding that in cardiomyoytes, sodium channel Nav1.5 is negatively regulated by Foxo1 (79). Intriguingly, this aspect of Foxo1 regulation suggests a positive feedback loop in which once Foxo1 is activated and begins to cause muscle atrophy the muscle also loses its ability to respond to stimulation, thus increasing its atrophy as seen in models of disuse and denervation.

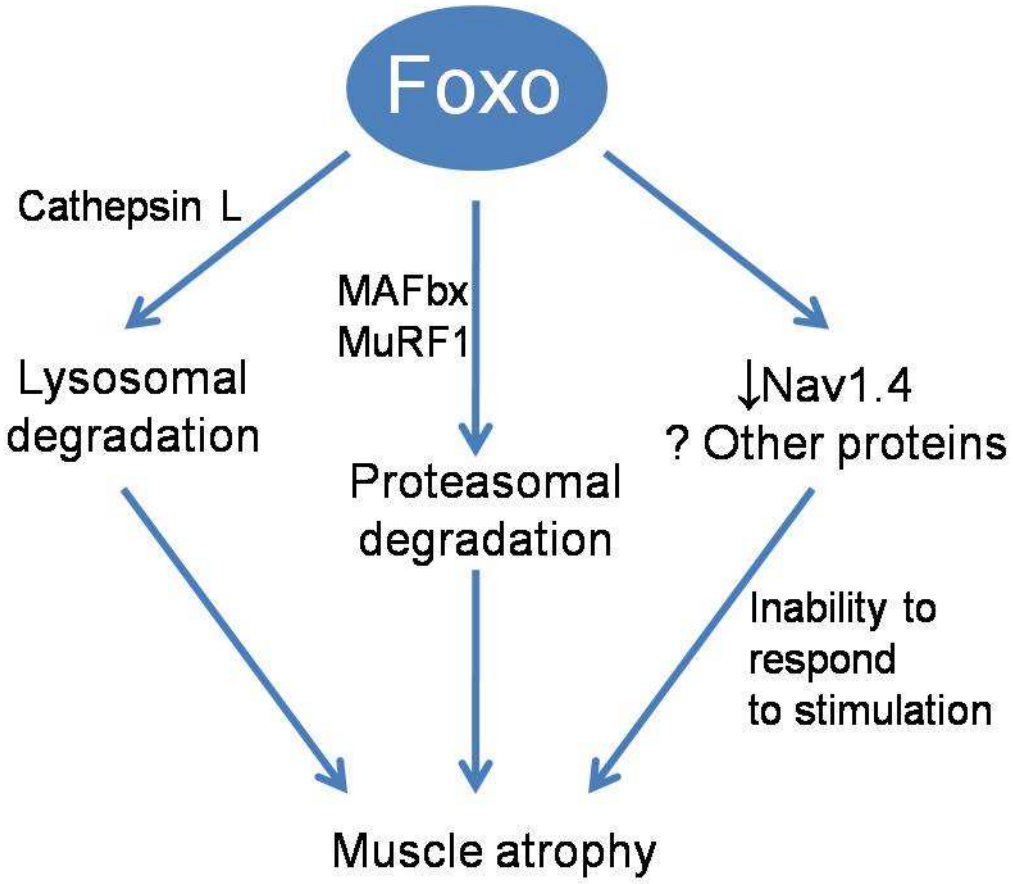

Figure 3.7 Foxo1 regulates muscle atrophy

Foxo1 regulates expression of proteins that carry out lysosomal degradation and proteasomal degradation leading to muscle atrophy. We demonstrate a novel method in which Foxo1 decreases the expression of sodium channel Nav1.4 and possibly other proteins that result in the inability of muscle fibers to respond to electrical stimulation. Lack of response to electrical stimulation and inability to contract as seen in denervation and disuse lead to muscle atrophy.

This system of overexpression of Foxo1 can also be used as a model for overactivity or dysregulation of Foxo1 and its effects on skeletal muscle because overexpression effectively mimics activation by increasing nuclear concentration as occurs during dyregulation of Foxo1. Although the role of Foxo1 in skeletal muscle is established as a regulator of both lysosomal and proteasomal degradation leading to muscle atrophy (56, 57, 60), we reveal that dysregulation of Foxo1 can also cause a disconnection between excitation of muscle and its ability to contract. Further understanding of the role of Foxo1 in muscle is now an even more attractive therapeutic avenue in treatment and prevention of muscle atrophy.

CHAPTER 4

CONCLUSIONS

The Foxo transcription factor family is integral to many processes including regulation of cell proliferation, cell cycle, and cell survival (6, 46). Foxo1 and Foxo3 play no less crucial of a role in skeletal muscle; both Foxo1 and Foxo3 regulate muscle size. As such, it is not surprising that these transcription factors have been the focus of much research. Target proteins that are expressed, as well as those that are not expressed due to Foxo regulation, have been identified. Regulators of Foxo activity have been studied and their mechanisms of actions established. Although so much is now understood, the field is not yet developed and the elusive therapeutic avenue to both reverse and prevent muscle atrophy has not yet been established.

To this end, we have developed a system in which to explore the function, regulation of Foxo, and regulation by Foxo in live muscle. Expression of Foxo-GFP fusion proteins in

cultured adult muscle fibers is an ideal setup that allows a real-time view of the dynamic processes that regulate Foxo as well as the effects of Foxo activity/inactivity. Foxo1-GFP and endogenous Foxo1 displayed consistent sub-sarcomeric distribution (**Figure 2.1**), nuclear/cytoplasmic localization (**Figure 2.2**), and translocation in response to phosphorylating intermediaries (**Figures 2.3, 2.4, and 2.5**).

Although other mechanisms of regulation of Foxo exist, phosphorylation is a major means by which Foxo activity is controlled. Exposure to IGF-1 results in phosphorylation and subsequent cytoplasmic retention, increasing cytoplasmic Foxo1 (**Figures 2.3 and 2.4** and reference 15). PI3K and Akt are also involved in the signaling pathway that results in phosphorylation of Foxo1 and its buildup in the cytoplasm (**Figure 2.4** and reference 24). Furthermore, Akt function is actually necessary for IGF-1 to induce cytoplasmic retention of Foxo1 (**Figure 2.10**). The functional role of the phosphatase PP2A was identified with the use of okadaic acid. PP2A dephosphorylates and promotes nuclear influx of Foxo1 (**Figure 2.5**). Additional experimentation further defined its position as being cytoplasmic (**Figure 2.6E**). PP2A may also have nuclear activity as well, but that aspect has not yet been explored.

At this point it is important to note that in this chapter, and the vast majority of papers discussing regulation of Foxo, the net movement of Foxo1 has been considered, with the exception of the work exploring cytoplasmic function of PP2A. However, here, we also calculate the unidirectional rate of nuclear influx by pharmacologically inhibiting nuclear efflux. An interesting extension of this project would be to develop a means by which to inhibit the nuclear import of Foxo and measuring the unidirectional rate of nuclear efflux. This could be done possibly by introducing a membrane-permeable peptide with an NLS

sequence that would act as a competitive inhibitor of Ran, and in this way prevent nuclear import. An alternative would be to use a pharmacological inhibitor of Ran. (Note that molecular means of knock down of Ran or siRNA would not be an efficient means of nuclear import inhibition for short experiments similar to what has been discussed in this work because it cannot be induced in a short period of time.) With the rate of nuclear import equal to zero, the net rate of change in nuclear Foxo1 would equal the rate of nuclear efflux. Using this method, we could determine if PP2A is a nuclear phosphatase as well as a cytoplasmic phosphatase. Inhibition of nuclear import would create the opportunity to determine the kinetics of nuclear efflux and thus elucidate the phosphorylating/dephosphorylating activities occurring in the nucleus in a similar manner to what we have established concerning cytoplasmic phosphorylation and nuclear import.

The data we have generated using LMB as a tool for isolation of the rate of nuclear influx has made the quantification of the effects of isolated phospholating/dephosphorylating events possible. Using the calculation of the apparent rate constant (k'; defined on page 49, eqn 1) we determine the effect of staurosporine to increase phosphorylated Foxo1 to 40% over basal levels and IGF-1 to decrease phosphorylated Foxo1 to a mere 11% of basal levels. This is an example of experimental treatment and data collection in combination with rigorous mathematical manipulation elucidating the kinetics of nuclear import as well as the cytoplasmic phosphorylation/dephosphorylation on which translocation is based.

Foxo1-GFP exhibits a high rate of nuclear-cytoplasmic shuttling under resting conditions. The high rates of unidirectional nuclear influx and efflux are in near balance under resting conditions, as determined by the unidirectional rate of nuclear influx and

unidirectional rate of nuclear efflux. Furthermore, the difference of the unidirectional rates of nuclear influx and efflux is equal to the net rate of nuclear influx (**Figure 2.7**). This further characterization of the Foxo1 nuclear-cytoplasmic shuttling system demonstrates again the unique capabilities of the system developed for exploration of Foxo in skeletal muscle.

Comparison of the kinetics of Foxo1 and Foxo3A revealed a 20-fold difference in the rates of nuclear influx (**Figure 2.8**). The much slower rate of nuclear influx of Foxo3A could be a result of a difference in the rate of phosphorylation of Foxo3A kinase due to a difference in the signaling that leads to phosphorylation or the binding efficiency of kinases that phosphorylate the different Foxo proteins. Another possibility is that Ran binds to Foxo1 and Foxo3A at different rates. A third possibility is that the fraction of unbound Foxo3A may be different from that of Foxo1. Possibly related to this finding is the discovery that Foxo1 and Foxo3A do not have the same sub-sarcomeric distribution (**Figure 2.1**). This would indicate that Foxo1 and Foxo3A are not bound to the same proteins in muscle fibers, and thus lends credence to the possibility that the fraction of unbound Foxo3A is significantly different from that of Foxo1.

The differences in nuclear-cytoplasmic shuttling coupled with the difference in sub-sarcomeric distribution bring the redundancy of Foxo transcription factors into question. Both Foxo1 and Foxo3A induce muscle atrophy (19, 38), however the differences that we have found in their regulation indicate that they may function- and even be regulated- in different ways. It would be very interesting to compare the impact of Foxo1 and the impact of Foxo3A on gene expression induction and prevention. Comparison of regulation of Foxo1 and Foxo3A would also help clarify the possibly diverse roles of

these proteins. Some other questions that we could answer are whether one isoform is preferentially nuclear and the other cytoplasmic? Do they have different cofactors? And, do they induce different phenotypes in skeletal muscle? Answering these questions and others will help our understanding of the components that regulate muscle size.

Our studies have revealed another phenotype in addition to muscle atrophy induced by Foxo1 activity. Overexpression of Foxo1 caused a lack of contraction or calcium transient in response to electrical stimulation that was prevented with IGF-1 treatment (**Figures 3.2 and 3.3**). The resting rates of calcium in control and Foxo1-GFP expressing fibers were essentially the same but Foxo1-GFP fibers did not have increased cellular calcium levels in response to electrical stimulation (**Figure 3.2 A-E**). These results indicate the involvement of Foxo1 in excitation of muscle. In order to ascertain the method by which Foxo1 impacts the muscle fiber's response to electrical stimulation we examined the morphology of the T-tubule system in fibers expressing exogenous Foxo1-GFP and determined that it was not altered or damaged in comparison to that of control fibers. This establishes that the lack of response is not due to the breakdown of the T-tubule system, which essentially acts as the circulatory system of individual fibers.

Using a voltage-dependent dye, we discovered that fibers expressing Foxo1-GFP was unable to propagate an action potential, thereby explaining the lack of response to electrical stimulation. But what prevented the propagation of the action potential? The cause of this malfunction was identified to be a decrease in the expression of the skeletal muscle sodium channel Nav1.4 (**Figure 3.6**). These surprising results give evidence of a novel mechanism by which Foxo1 induces muscle atrophy (**Figure 3.7**) as well as an

additional function of Foxo1 besides muscle atrophy- an involvement in depolarization of muscle.

Our understanding of the roles and regulation of the Foxo transcription factors has come a long way. Pathways of activation and inhibition of these proteins have been identified as well as binding partners and target genes whose expression are induced or prevented due to Foxo activity. Cellular processes that Foxo proteins are involved in have been identified. Roles of cell-specific activity and cell-specific expression of different isoforms have been distinguished. However, there are still many questions left to be answered in this field that have the potential to be crucial in the development of treatment and possibly even prevention of muscle atrophy.

SCHOLARLY REFERENCES

1. Weigel D, Jurgens G, Kuttner F, Seifert E & Jackle H (1989) The homeotic gene fork head encodes a nuclear protein and is expressed in the terminal regions of the drosophila embryo. *Cell* 57: 645-658.

2. Galili N, *et al* (1993) Fusion of a fork head domain gene to PAX3 in the solid tumour alveolar rhabdomyosarcoma. *Nat Genet* 5: 230-235.

3. Obsil T & Obsilova V (2008) Structure/function relationships underlying regulation of FOXO transcription factors. *Oncogene* 27: 2263-2275.

4. Clark KL, Halay ED, Lai E & Burley SK (1993) Co-crystal structure of the HNF-3/fork head DNA-recognition motif resembles histone H5. *Nature* 364: 412-420.

5. Biggs WH,3rd, Cavenee WK & Arden KC (2001) Identification and characterization of members of the FKHR (FOX O) subclass of winged-helix transcription factors in the mouse. *Mamm Genome* 12: 416-425.

6. Arden KC & Biggs WH,3rd (2002) Regulation of the FoxO family of transcription factors by phosphatidylinositol-3 kinase-activated signaling. *Arch Biochem Biophys* 403: 292-298.

7. Brunet A, *et al* (1999) Akt promotes cell survival by phosphorylating and inhibiting a forkhead transcription factor. *Cell* 96: 857-868.

8. Rena G, Guo S, Cichy SC, Unterman TG & Cohen P (1999) Phosphorylation of the transcription factor forkhead family member FKHR by protein kinase B. *J Biol Chem* 274: 17179-17183.

9. Brunet A, *et al* (2001) Protein kinase SGK mediates survival signals by phosphorylating the forkhead transcription factor FKHRL1 (FOXO3a). *Mol Cell Biol* 21: 952-965.

10. Rena G, *et al* (2002) Two novel phosphorylation sites on FKHR that are critical for its nuclear exclusion. *EMBO J* 21: 2263-2271.

11. Woods YL, *et al* (2001) The kinase DYRK1A phosphorylates the transcription factor FKHR at Ser329 in vitro, a novel in vivo phosphorylation site. *Biochem J* 355: 597-607.

12. Burgering BM & Medema RH (2003) Decisions on life and death: FOXO forkhead transcription factors are in command when PKB/Akt is off duty. *J Leukoc Biol* 73: 689-701.

13. Singh A, *et al* (2010) Protein phosphatase 2A reactivates FOXO3a through a dynamic interplay with 14-3-3 and AKT. *Mol Biol Cell* 21: 1140-1152.

14. Yan L, *et al* (2008) PP2A regulates the pro-apoptotic activity of FOXO1. *J Biol Chem* 283: 7411-7420.

15. Zhang X, *et al* (2002) Phosphorylation of serine 256 suppresses transactivation by FKHR (FOXO1) by multiple mechanisms. direct and indirect effects on nuclear/cytoplasmic shuttling and DNA binding. *J Biol Chem* 277: 45276-45284.

16. Nakae J, Barr V & Accili D (2000) Differential regulation of gene expression by insulin and IGF-1 receptors correlates with phosphorylation of a single amino acid residue in the forkhead transcription factor FKHR. *EMBO J* 19: 989-996.

17. Zhao X, *et al* (2004) Multiple elements regulate nuclear/cytoplasmic shuttling of FOXO1: Characterization of phosphorylation- and 14-3-3-dependent and -independent mechanisms. *Biochem J* 378: 839-849.

18. Brownawell AM, Kops GJ, Macara IG & Burgering BM (2001) Inhibition of nuclear import by protein kinase B (akt) regulates the subcellular distribution and activity of the forkhead transcription factor AFX. *Mol Cell Biol* 21: 3534-3546.

19. Sandri M, *et al* (2004) Foxo transcription factors induce the atrophy-related ubiquitin ligase atrogin-1 and cause skeletal muscle atrophy. *Cell* 117: 399-412.

20. Florini JR, Ewton DZ & Coolican SA (1996) Growth hormone and the insulin-like growth factor system in myogenesis. *Endocr Rev* 17: 481-517.

21. Cantley LC (2002) The phosphoinositide 3-kinase pathway. *Science* 296: 1655-1657.

22. Downward J (1998) Mechanisms and consequences of activation of protein kinase B/Akt. *Curr Opin Cell Biol* 10: 262-267.

23. Vivanco I & Sawyers CL (2002) The phosphatidylinositol 3-kinase AKT pathway in human cancer. *Nat Rev Cancer* 2: 489-501.

24. Hribal ML, Nakae J, Kitamura T, Shutter JR & Accili D (2003) Regulation of insulin-like growth factor-dependent myoblast differentiation by foxo forkhead transcription factors. *J Cell Biol* 162: 535-541.

25. Mammucari C, *et al* (2007) FoxO3 controls autophagy in skeletal muscle in vivo. *Cell Metab* 6: 458-471.

26. Alessi DR (2001) Discovery of PDK1, one of the missing links in insulin signal transduction. colworth medal lecture. *Biochem Soc Trans* 29: 1-14.

27. Collins BJ, Deak M, Arthur JS, Armit LJ & Alessi DR (2003) In vivo role of the PIF-binding docking site of PDK1 defined by knock-in mutation. *EMBO J* 22: 4202-4211.

28. Graves PR & Roach PJ (1995) Role of COOH-terminal phosphorylation in the regulation of casein kinase I delta. *J Biol Chem* 270: 21689-21694.

29. Flotow H, *et al* (1990) Phosphate groups as substrate determinants for casein kinase I action. *J Biol Chem* 265: 14264-14269.

30. Becker W, *et al* (1998) Sequence characteristics, subcellular localization, and substrate specificity of DYRK-related kinases, a novel family of dual specificity protein kinases. *J Biol Chem* 273: 25893-25902.

31. De Ruiter ND, Burgering BM & Bos JL (2001) Regulation of the forkhead transcription factor AFX by ral-dependent phosphorylation of threonines 447 and 451. *Mol Cell Biol* 21: 8225-8235.

32. Brunet A, *et al* (2004) Stress-dependent regulation of FOXO transcription factors by the SIRT1 deacetylase. *Science* 303: 2011-2015.

33. Fukuoka M, *et al* (2003) Negative regulation of forkhead transcription factor AFX (Foxo4) by CBP-induced acetylation. *Int J Mol Med* 12: 503-508.

34. Motta MC, *et al* (2004) Mammalian SIRT1 represses forkhead transcription factors. *Cell* 116: 551-563.

35. Matsuzaki H, Daitoku H, Hatta M, Tanaka K & Fukamizu A (2003) Insulin-induced phosphorylation of FKHR (Foxo1) targets to proteasomal degradation. *Proc Natl Acad Sci U S A* 100: 11285-11290.

36. Huang H, *et al* (2005) Skp2 inhibits FOXO1 in tumor suppression through ubiquitin-mediated degradation. *Proc Natl Acad Sci U S A* 102: 1649-1654.

37. Jacobs FM, *et al* (2003) FoxO6, a novel member of the FoxO class of transcription factors with distinct shuttling dynamics. *J Biol Chem* 278: 35959-35967.

38. Kamei Y, *et al* (2004) Skeletal muscle FOXO1 (FKHR) transgenic mice have less skeletal muscle mass, down-regulated type I (slow twitch/red muscle) fiber genes, and impaired glycemic control. *J Biol Chem* 279: 41114-41123.

39. Hosaka T, *et al* (2004) Disruption of forkhead transcription factor (FOXO) family members in mice reveals their functional diversification. *Proc Natl Acad Sci U S A* 101: 2975-2980.

40. Moylan JS, Smith JD, Chambers MA, McLoughlin TJ & Reid MB (2008) TNF induction of atrogin-1/MAFbx mRNA depends on Foxo4 expression but not AKT-Foxo1/3 signaling. *Am J Physiol Cell Physiol* 295: C986-93.

41. Kops GJ, *et al* (1999) Direct control of the forkhead transcription factor AFX by protein kinase B. *Nature* 398: 630-634.

42. Takaishi H, *et al* (1999) Regulation of nuclear translocation of forkhead transcription factor AFX by protein kinase B. *Proc Natl Acad Sci U S A* 96: 11836-11841.

43. Pardo PS, Lopez MA & Boriek AM (2008) FOXO transcription factors are mechanosensitive and their regulation is altered with aging in the respiratory pump. *Am J Physiol Cell Physiol* 294: C1056-66.

44. Wen Q, *et al* (2011) Characterization of intracellular translocation of forkhead transcription factor O (FoxO) members induced by NGF in PC12 cells. *Neurosci Lett* 498: 31-36.

45. Furuyama T, Kitayama K, Yamashita H & Mori N (2003) Forkhead transcription factor FOXO1 (FKHR)-dependent induction of PDK4 gene expression in skeletal muscle during energy deprivation. *Biochem J* 375: 365-371.

46. Puig O & Tjian R (2006) Nutrient availability and growth: Regulation of insulin signaling by dFOXO/FOXO1. *Cell Cycle* 5: 503-505.

47. Stitt TN, *et al* (2004) The IGF-1/PI3K/Akt pathway prevents expression of muscle atrophy-induced ubiquitin ligases by inhibiting FOXO transcription factors. *Mol Cell* 14: 395-403.

48. Tothova Z, *et al* (2007) FoxOs are critical mediators of hematopoietic stem cell resistance to physiologic oxidative stress. *Cell* 128: 325-339.

49. Nehls M, Pfeifer D, Schorpp M, Hedrich H & Boehm T (1994) New member of the winged-helix protein family disrupted in mouse and rat nude mutations. *Nature* 372: 103-107.

50. Kamei Y, *et al* (2003) A forkhead transcription factor FKHR up-regulates lipoprotein lipase expression in skeletal muscle. *FEBS Lett* 536: 232-236.

51. Bois PR & Grosveld GC (2003) FKHR (FOXO1a) is required for myotube fusion of primary mouse myoblasts. *EMBO J* 22: 1147-1157.

52. Furuyama T, *et al* (2002) Effects of aging and caloric restriction on the gene expression of Foxo1, 3, and 4 (FKHR, FKHRL1, and AFX) in the rat skeletal muscles. *Microsc Res Tech* 59: 331-334.

53. McLoughlin TJ, *et al* (2009) FoxO1 induces apoptosis in skeletal myotubes in a DNA-binding-dependent manner. *Am J Physiol Cell Physiol* 297: C548-55.

54. Lecker SH, Goldberg AL & Mitch WE (2006) Protein degradation by the ubiquitin-proteasome pathway in normal and disease states. *J Am Soc Nephrol* 17: 1807-1819.

55. Lum JJ, DeBerardinis RJ & Thompson CB (2005) Autophagy in metazoans: Cell survival in the land of plenty. *Nat Rev Mol Cell Biol* 6: 439-448.

56. Bodine SC, *et al* (2001) Identification of ubiquitin ligases required for skeletal muscle atrophy. *Science* 294: 1704-1708.

57. Lecker SH, Solomon V, Mitch WE & Goldberg AL (1999) Muscle protein breakdown and the critical role of the ubiquitin-proteasome pathway in normal and disease states. *J Nutr* 129: 227S-237S.

58. Du J, *et al* (2004) Activation of caspase-3 is an initial step triggering accelerated muscle proteolysis in catabolic conditions. *J Clin Invest* 113: 115-123.

59. Kramerova I, Kudryashova E, Venkatraman G & Spencer MJ (2005) Calpain 3 participates in sarcomere remodeling by acting upstream of the ubiquitin-proteasome pathway. *Hum Mol Genet* 14: 2125-2134.

60. Zhao J, *et al* (2007) FoxO3 coordinately activates protein degradation by the autophagic/lysosomal and proteasomal pathways in atrophying muscle cells. *Cell Metab* 6: 472-483.

61. Block BA, Imagawa T, Campbell KP & Franzini-Armstrong C (1988) Structural evidence for direct interaction between the molecular components of the transverse tubule/sarcoplasmic reticulum junction in skeletal muscle. *J Cell Biol* 107: 2587-2600.

62. Rios E & Brum G (1987) Involvement of dihydropyridine receptors in excitation-contraction coupling in skeletal muscle. *Nature* 325: 717-720.

63. Schneider MF & Chandler WK (1973) Voltage dependent charge movement of skeletal muscle: A possible step in excitation-contraction coupling. *Nature* 242: 244-246.

64. Hodgkin AL & Huxley AF (1952) Movement of sodium and potassium ions during nervous activity. *Cold Spring Harb Symp Quant Biol* 17: 43-52.

65. Horowicz P & Schneider MF (1981) Membrane charge moved at contraction thresholds in skeletal muscle fibres. *J Physiol* 314: 595-633.

66. Liu Y, Contreras M, Shen T, Randall WR & Schneider MF (2009) Alpha-adrenergic signalling activates protein kinase D and causes nuclear efflux of the transcriptional repressor HDAC5 in cultured adult mouse soleus skeletal muscle fibres. *J Physiol* 587: 1101-1115.

67. Ni YG, *et al* (2006) Foxo transcription factors blunt cardiac hypertrophy by inhibiting calcineurin signaling. *Circulation* 114: 1159-1168.

68. Shen T, *et al* (2010) DNA binding sites target nuclear NFATc1 to heterochromatin regions in adult skeletal muscle fibers. *Histochem Cell Biol* 134: 387-402.

69. Shen T, Liu Y & Schneider MF (2012) Localization and regulation of the N terminal splice variant of PGC-1alpha in adult skeletal muscle fibers. *J Biomed Biotechnol* 2012: 989263.

70. Coolican SA, Samuel DS, Ewton DZ, McWade FJ & Florini JR (1997) The mitogenic and myogenic actions of insulin-like growth factors utilize distinct signaling pathways. *J Biol Chem* 272: 6653-6662.

71. Perrone CE, Fenwick-Smith D & Vandenburgh HH (1995) Collagen and stretch modulate autocrine secretion of insulin-like growth factor-1 and insulin-like growth factor binding proteins from differentiated skeletal muscle cells. *J Biol Chem* 270: 2099-2106.

72. Bain J, *et al* (2007) The selectivity of protein kinase inhibitors: A further update. *Biochem J* 408: 297-315.

73. Barnett SF, *et al* (2005) Identification and characterization of pleckstrin-homology-domain-dependent and isoenzyme-specific akt inhibitors. *Biochem J* 385: 399-408.

74. Tanuma N, *et al* (2008) Nuclear inhibitor of protein phosphatase-1 (NIPP1) directs protein phosphatase-1 (PP1) to dephosphorylate the U2 small nuclear ribonucleoprotein particle (snRNP) component, spliceosome-associated protein 155 (Sap155). *J Biol Chem* 283: 35805-35814.

75. Hedrick SM (2009) The cunning little vixen: Foxo and the cycle of life and death. *Nat Immunol* 10: 1057-1063.

76. Shen T, Liu Y, Randall WR & Schneider MF (2006) Parallel mechanisms for resting nucleo-cytoplasmic shuttling and activity dependent translocation provide dual control of transcriptional regulators HDAC and NFAT in skeletal muscle fiber type plasticity. *J Muscle Res Cell Motil* 27: 405-411.

77. Schachter TN, Shen T, Liu Y & Schneider MF (2012) Kinetics of nuclear-cytoplasmic translocation of Foxo1 and Foxo3A in adult skeletal muscle fibers. *Am J Physiol Cell Physiol*

78. Prosser BL, *et al* (2010) S100A1 promotes action potential-initiated calcium release flux and force production in skeletal muscle. *Am J Physiol Cell Physiol* 299: C891-902.

79. Mao W, *et al* (2012) Reactive oxygen species suppress cardiac NaV1.5 expression through Foxo1. *PLoS One* 7: e32738.